OPEN ACCESS

Haya: The Saudi Journal of Life Sciences

Abbreviated Key Title: Haya Saudi J Life Sci
ISSN 2415-623X (Print) | ISSN 2415-6221 (Online)
Scholars Middle East Publishers, Dubai, United Arab Emirates
Journal homepage: https://saudijournals.com

Original Research Article

From CO_2 Capture to Energy Conversion: Nanostructured Metals, Plasmonic Nanoparticles, Quantum Dots, and Defective Tio_2 for CO_2 → CO / CH_4 / CH_3OH Reactions in Catalysis, Photovoltaics, and Optoelectronics

Muhammad Asad[1], Usama Shahab[2], Muhammad Umar Farooq Ahmad[3], Nawa Arshad[4], Muhammad Azam Shani[2], Abbas Abubakar[5], Shaima Muzammil[6], Muhammad Farooq[7], Iqra Rizwan[8], Khalid Khan[9]*

[1]School of Chemistry, Xi'an Jiaotong University, China
[2]Department of Physics, Riphah International University, Pakistan
[3]Department of Chemical Engineering, Comsats University Islamabad, Lahore Campus, Pakistan
[4]Department of Physics, University of Agriculture Faisalabad, Pakistan
[5]Department of Chemical and Biomolecular Engineering, Tulane University, USA
[6]Department of Physics, Comsats University Islamabad
[7]Department of Chemistry, University of Sahiwal, Punjab, Pakistan
[8]Institute of Chemical Sciences, Bahauddin Zakariya University, Multan, Pakistan
[9]Department of Chemistry, Kohat University of Science and Technology, Kohat

DOI: https://doi.org/10.36348/sjls.2026.v11i02.004 | **Received:** 16.12.2025 | **Accepted:** 12.02.2026 | **Published:** 14.02.2026

***Corresponding author:** Khalid Khan
Department of Chemistry, Kohat University of Science and Technology, Kohat

Abstract

The persistent increase in atmospheric CO_2 levels presents a dual challenge of environmental mitigation and sustainable energy generation. This study introduces a unified nano-engineered platform combining nanostructured metals, plasmonic nanoparticles, quantum dots, and defect-rich TiO_2 to drive selective CO_2 conversion into CO, CH_4, and CH_3OH. By leveraging synergistic nano-interfaces, this work integrates catalytic activity with optoelectronic functionality, enabling simultaneous energy harvesting and chemical transformation. Nanostructured metals provide tailored surface states for CO_2 adsorption, while plasmonic nanoparticles induce hot-electron injection, and quantum dots facilitate directional charge transfer. Defective TiO_2 layers introduce oxygen vacancies that localize charges and modulate reaction pathways. Comprehensive material characterization using TEM, XRD, XPS, PL, and UV–Vis spectroscopy confirms controlled interface formation, defect density, and optical enhancement. CO_2 conversion experiments under gas-phase and photo-assisted modes demonstrate tunable product selectivity via defect engineering and electrical bias application. The hybrid platform achieves enhanced Faradaic efficiency, turnover number, and operational stability compared to conventional systems. Mechanistic insights reveal that defect-plasmon-quantum dot interactions govern charge localization and transfer, providing a predictive framework for reaction steering. Integration with photovoltaic and optoelectronic modules showcases the feasibility of combined chemical and energy conversion, offering a pathway toward scalable, smart CO_2-to-fuel system. These findings provide a transformative approach to CO_2 utilization, highlighting the potential for decentralized renewable energy generation and sustainable fuel production. The methodology and insights reported herein establish a foundation for designing multi-functional catalytic systems with controllable reaction pathways and integrated energy recovery.

Keywords: CO_2 reduction, Nanostructured metals, Plasmonic nanoparticles, Quantum dots, Defective TiO_2.

1. INTRODUCTION

Carbon dioxide conversion has transitioned from an environmental mitigation concept to a strategic energy research frontier. Rather than treating CO_2 as an unavoidable emission, emerging perspectives recognize it as a chemically stable yet abundant carbon reservoir that can be deliberately activated and transformed. However, the complexity of CO_2 utilization lies in its multiscale nature, spanning molecular activation, interfacial charge transport, and system-level energy management. Addressing these dimensions in isolation has yielded incremental progress but has failed to deliver

transformative performance. This study adopts a holistic framework in which CO_2 capture, catalytic conversion, and energy harvesting are treated as interconnected processes governed by coupled electronic and photonic phenomena. By structuring the investigation around material synergy rather than individual functionality, the present work establishes a coherent pathway from fundamental reaction barriers to device-level energy conversion outcomes [1,2,166].

1.1 Global CO_2 Challenge and Energy Conversion Imperative

Carbon dioxide has emerged as one of the most persistent thermodynamic sinks in modern energy systems. Its linear molecular structure and strong C=O bonds render it chemically stable, making spontaneous activation highly unfavorable under ambient conditions. As a result, CO_2 accumulation continues to rise despite decades of mitigation strategies, positioning it simultaneously as an environmental liability and a dormant carbon resource. The central challenge is not merely capturing CO_2, but converting it into value-added products through energetically feasible and selective pathways [3,4].

From a kinetic perspective, CO_2 reduction reactions are hindered by high activation barriers and competitive side reactions. Conventional thermal catalysis often demands elevated temperatures and pressures, which compromise energy efficiency and long-term material stability. Electrochemical routes, while promising, suffer from poor selectivity and limited scalability when operated as isolated systems. These limitations collectively highlight that CO_2 conversion is not a single-step problem, but a multi-stage process involving capture, activation, charge transfer, and product desorption. Current CO_2 capture technologies, including amine scrubbing and physical adsorption, remain largely decoupled from downstream utilization. This separation introduces energy penalties due to compression, transport, and regeneration steps. More critically, captured CO_2 is rarely converted in situ, leading to system-level inefficiencies. These drawbacks expose a fundamental design flaw: capture and conversion are treated as independent processes rather than components of a unified energy platform.

An integrated capture–conversion–energy framework is therefore essential. Such a framework must simultaneously address molecular activation, reaction selectivity, and energy harvesting. The convergence of catalysis with photovoltaic and optoelectronic functionalities offers a viable pathway toward this integration. By harnessing photonic energy and electronically tunable interfaces, CO_2 conversion can be driven under milder conditions with improved selectivity control [5-7].

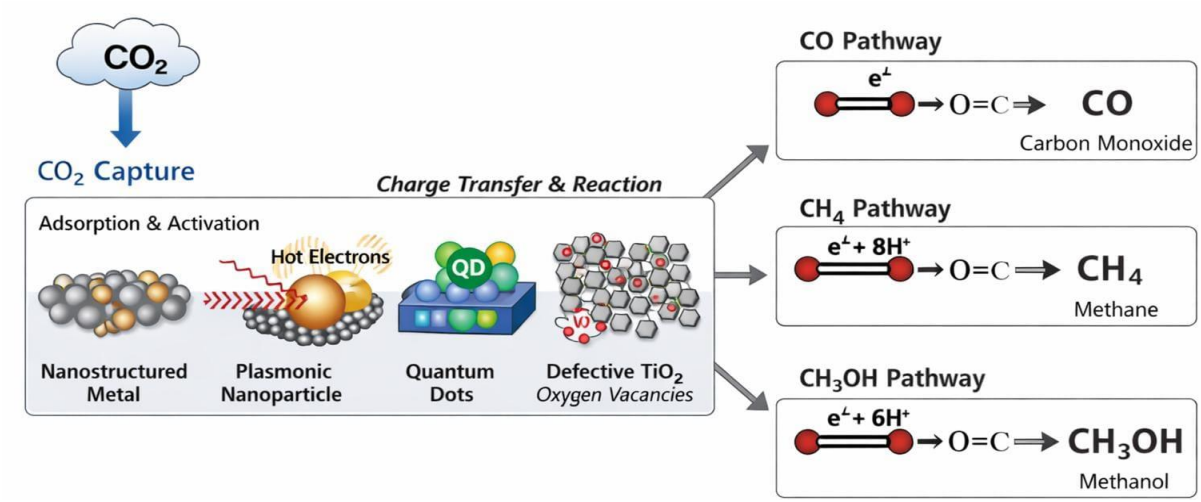

Figure 1. Schematic of CO_2 capture and selective conversion to CO, CH_4, and CH_3OH via integrated nano-interfaces.

Conceptual schematic illustrating CO_2 capture, molecular activation, and selective multi-pathway conversion toward CO, CH_4, and CH_3OH through coupled catalytic, photovoltaic, and optoelectronic processes.

Among potential reduction products, carbon monoxide (CO), methane (CH_4), and methanol (CH_3OH) occupy strategic positions in the energy landscape. CO serves as a critical feedstock for Fischer–Tropsch synthesis and syngas chemistry. CH_4 represents a high-energy-density fuel compatible with existing infrastructure. CH_3OH functions as both a liquid fuel and a versatile chemical intermediate. Importantly, these products arise from distinct reaction pathways, each governed by different electron-proton transfer sequences and surface binding energetics. The ability to selectively direct CO_2 toward CO, CH_4, or CH_3OH within a single

platform would constitute a transformative advance. Achieving this requires precise control over charge localization, reaction intermediates, and energy input modes. Consequently, the focus must shift from isolated catalytic activity toward system-level reaction pathway engineering [8,9].

1.2 Nanostructured Materials as Catalytic and Photo-Active Platforms

Nanostructured materials provide a unique opportunity to overcome the thermodynamic and kinetic barriers associated with CO_2 conversion. At the nanoscale, surface-to-volume ratios increase dramatically, exposing under-coordinated atoms and tunable electronic states. These features are particularly advantageous for stabilizing reaction intermediates and lowering activation energies [10-15].

Nanostructured metals play a critical role in this context due to their adjustable surface states and d-band centers. By tailoring particle size, morphology, and crystallographic orientation, adsorption energies of key intermediates such as *COOH and *CHO can be modulated. This enables preferential reaction pathways to be activated while suppressing undesired side reactions. However, metallic catalysts alone often lack sufficient control over photonic energy utilization.

Plasmonic nanoparticles introduce an additional dimension through localized surface plasmon resonance. Upon light excitation, collective electron oscillations generate non-equilibrium hot carriers capable of driving endergonic surface reactions. These hot electrons can transiently populate antibonding orbitals of adsorbed CO_2 molecules, facilitating bond bending and activation. Despite this advantage, plasmonic systems suffer from rapid carrier relaxation unless coupled with suitable charge acceptors [16-19].

Quantum dots offer precisely this capability. Their size-dependent band structures allow fine control over energy level alignment with adjacent materials. When integrated with plasmonic or catalytic components, quantum dots act as charge mediators, prolonging carrier lifetimes and enhancing interfacial charge transfer. This property is particularly valuable for directing multi-electron reduction pathways required for CH_4 and CH_3OH formation.

Defective titanium dioxide further complements this material ensemble. Oxygen vacancies introduce mid-gap states that serve as electron traps and adsorption sites for CO_2. These defects enhance visible-light absorption and improve charge separation efficiency. More importantly, defect density can be deliberately tuned, offering a handle to regulate reaction kinetics and selectivity [20-26].

Individually, nanostructured metals, plasmonic nanoparticles, quantum dots, and defective TiO_2 have demonstrated partial success in CO_2 reduction. However, their true potential lies in synergistic integration. When engineered as coupled nano-interfaces, these materials can collectively manage photon absorption, charge generation, carrier transport, and catalytic conversion within a single architecture.

Table 1. Comparison of nanostructured material classes in CO_2 conversion systems.

Material Class	Primary Function	Reaction Bias	Energy Domain
Nanostructured metals	Surface catalysis	CO / CH_4	Thermal / Electrochemical
Plasmonic nanoparticles	Hot-electron generation	CO	Photonic
Quantum dots	Band alignment control	CH_4 / CH_3OH	Optoelectronic
Defective TiO_2	Charge trapping, adsorption	CH_3OH	Photocatalytic

1.3 Research Gap and Hypothesis

Despite substantial progress, existing CO_2 conversion studies remain fragmented. Most investigations focus on a single material class or energy input mode. Catalysts are optimized independently of light-harvesting components. Photovoltaic systems are rarely integrated with reaction selectivity control. As a result, performance gains achieved in isolated domains fail to translate into scalable, multifunctional platforms.

The missing link is cross-domain coupling. Specifically, there is a lack of systematic strategies that merge catalysis, photovoltaics, and optoelectronics into a unified CO_2 conversion system. Without this integration, charge carriers generated through photonic excitation cannot be efficiently directed toward targeted chemical pathways. This disconnect fundamentally limits selectivity and energy efficiency.

In response, this work advances the hypothesis that synergistic nano-interfaces can actively steer CO_2 reaction pathways through coordinated electronic and photonic coupling. By integrating nanostructured metals, plasmonic nanoparticles, quantum dots, and defective TiO_2 within a single architecture, it becomes possible to manipulate charge localization, intermediate stabilization, and energy flow in real time.

The proposed system is not designed to maximize a single product yield. Instead, it introduces a tunable platform where CO, CH_4, and CH_3OH formation can be selectively promoted by adjusting defect density,

plasmonic excitation, and optoelectronic bias. This represents a shift from catalyst-centric optimization toward pathway-centric engineering [27-38].

2. LITERATURE REVIEW

Despite rapid growth in CO_2 reduction research, the field remains structurally fragmented. Most studies emphasize incremental material improvements without addressing system-level coherence between energy input, charge transport, and reaction selectivity. As a result, reported efficiencies and selectivities often lack transferability beyond controlled laboratory conditions. This section critically examines state-of-the-art nanostructured and photo-active CO_2 conversion systems, not to catalogue prior work, but to identify unresolved limitations that motivate the integrated approach proposed in this study.

2.1 CO_2 Reduction on Nanostructured and Plasmonic Catalysts

Nanostructured catalysts have been extensively explored for CO_2 reduction due to their enhanced surface reactivity and tunable electronic properties. Metallic nanostructures such as Cu, Ag, Au, and their alloys dominate the literature, primarily because of their ability to stabilize key intermediates during CO_2 activation. Performance benchmarks reported in recent Q1 studies often highlight high current densities and improved Faradaic efficiencies, particularly for CO formation on Ag- and Au-based nanostructures. However, these metrics are typically optimized under narrowly defined conditions, limiting broader applicability. A persistent challenge across nanostructured metal catalysts is reaction selectivity. Copper-based systems, for instance, exhibit the ability to produce hydrocarbons such as CH_4, yet often suffer from competing hydrogen evolution reactions. Selectivity windows remain narrow, requiring precise control over surface morphology, electrolyte composition, and applied potential. Even minor deviations result in significant product redistribution, underscoring the instability of purely catalytic control strategies [39-43].

Plasmonic nanoparticles have been introduced as a means to overcome kinetic barriers through photonic activation. Upon light excitation, localized surface plasmon resonance generates energetic charge carriers capable of driving otherwise unfavorable reactions. Several studies report enhanced CO_2 conversion rates under illumination, attributing these gains to hot-electron injection into adsorbed CO_2 molecules. While promising, such enhancements are often transient. Rapid carrier relaxation and recombination severely limit sustained reaction control.

The coexistence of thermal and photonic activation further complicates system behavior. In many reported plasmonic systems, it remains unclear whether observed improvements arise from true hot-carrier chemistry or from localized photothermal heating. This ambiguity undermines mechanistic clarity and makes rational design difficult. Moreover, photon-driven activation is rarely synchronized with catalytic surface states, resulting in inefficient energy utilization. Crucially, most nanostructured and plasmonic catalyst studies treat CO_2 reduction as an isolated surface reaction. The absence of integrated charge management and downstream energy extraction prevents these systems from evolving into multifunctional energy platforms. As a result, state-of-the-art performance benchmarks, while impressive on paper, remain confined to single-domain optimization.

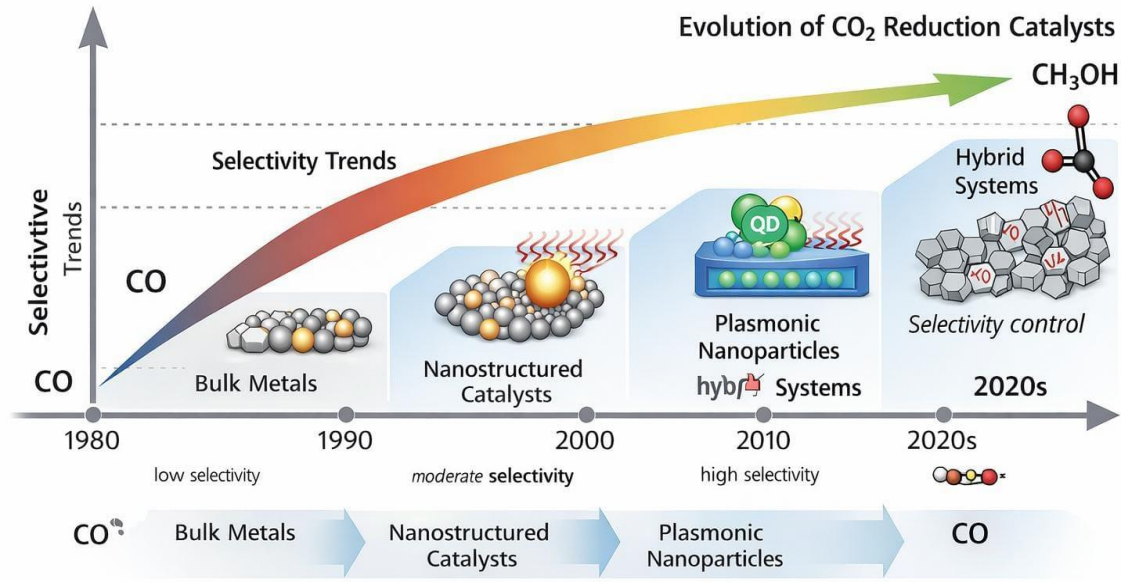

Figure 2. Timeline of CO_2 reduction catalyst evolution and selectivity trends toward CO, CH_4, and CH_3OH.

This timeline contextualizes how catalyst development has progressed from bulk metals to nanostructured and plasmonic systems. Despite improved activity, selectivity control remains inconsistent, emphasizing the need for cross-domain integration rather than further material isolation [44].

2.2 Quantum Dots and Defective TiO_2 in Photo-Driven CO_2 Conversion

Photo-driven CO_2 conversion has gained traction as a strategy to utilize renewable energy directly. Quantum dots have emerged as attractive components due to their discrete energy levels and size-dependent band gaps. These properties allow precise alignment with adjacent catalytic materials, theoretically enabling efficient charge separation and directional electron transfer. Several studies demonstrate enhanced CO_2 reduction under visible light when quantum dots are coupled to metal catalysts or oxide supports [45-48].

However, the benefits of quantum dots are often constrained by interfacial losses. Charge carriers generated within quantum dots frequently recombine before participating in surface reactions, particularly in systems lacking engineered charge extraction pathways. Stability also poses a challenge, as prolonged illumination can degrade quantum dot structures, reducing long-term performance.

Defective TiO_2 represents another extensively studied photo-active material. Oxygen vacancies introduce localized electronic states that improve CO_2 adsorption and extend light absorption into the visible spectrum. These defects can stabilize reaction intermediates and facilitate multi-electron transfer processes, which are essential for CH_3OH formation. Yet, defect engineering introduces its own limitations. Excessive defect densities promote recombination, while insufficient defects fail to provide meaningful enhancement. A common shortcoming across quantum dot and defective TiO_2 systems is their operation as standalone photocatalysts. While light absorption and charge generation are demonstrated, few studies integrate these processes with controlled catalytic selectivity or energy harvesting mechanisms. Consequently, reported efficiencies remain modest, and reaction pathways are weakly regulated. Most notably, optoelectronic integration is largely absent from existing designs. Photogenerated charges are rarely directed toward external circuits or coupled with bias-controlled reaction steering. This omission represents a critical gap, as optoelectronic coupling could provide dynamic control over reaction energetics and selectivity [49].

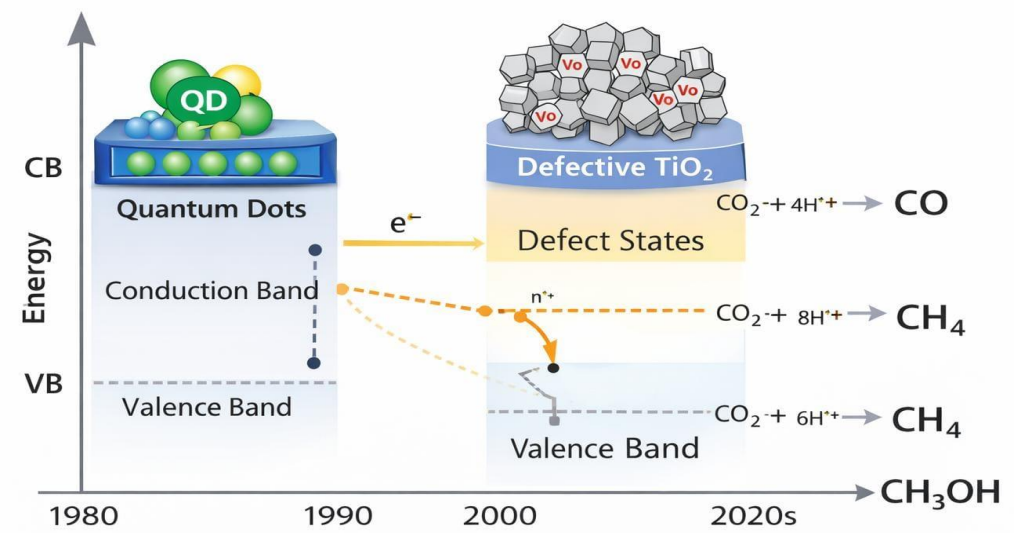

Figure 3. Energy band alignment and charge transfer pathways in quantum dot–defective TiO_2 systems.

This schematic highlights how band alignment governs charge separation efficiency. While favorable alignment enables electron transfer, the absence of external charge management limits sustained CO_2 reduction performance.

Table 2. Performance metrics of representative Q1 studies on photo-driven CO_2 conversion.

System Type	Product	TON	Faradaic Efficiency (%)	Stability (h)
QD–Metal Hybrid	CO	Moderate	40–60	<10
Defective TiO_2	CH_3OH	Low–Moderate	20–35	12–24
Plasmonic Oxide	CO	Moderate	30–50	<8

The table reveals that while diverse material systems achieve measurable CO_2 conversion, none simultaneously deliver high selectivity, stability, and energy efficiency. This reinforces the need for integrated design strategies [50-58].

Why Existing Literature Falls Short

Across nanostructured metals, plasmonic nanoparticles, quantum dots, and defective oxides, a common pattern emerges. Materials are optimized within disciplinary silos, leading to localized performance improvements but limited system coherence. Reaction selectivity is treated as a surface phenomenon, energy input as an external parameter, and charge transport as a secondary concern.

This fragmented approach prevents dynamic control over CO_2 reaction pathways. Without coupling catalytic interfaces to photovoltaic and optoelectronic frameworks, photogenerated charges cannot be efficiently directed, stored, or extracted. Consequently, existing systems lack adaptability and fail to transition from proof-of-concept demonstrations to scalable energy solutions. The present study addresses this limitation by reframing CO_2 conversion as an integrated energy process. Rather than advancing another isolated material, it proposes a synergistic nano-interface architecture where catalytic activity, photonic excitation, and electronic control operate in concert. This shift in design philosophy forms the foundation for the methodology and results presented in the following sections.

3. METHODOLOGY

The methodological framework of this study is designed to ensure both originality and reproducibility while enabling controlled investigation of synergistic nano-interface effects on CO_2 conversion. Rather than optimizing isolated materials, the methodology emphasizes interface engineering, defect regulation, and optoelectronic coupling. Each experimental step is selected to allow direct correlation between structural features, charge dynamics, and reaction selectivity, thereby supporting mechanistic interpretation alongside performance evaluation [59-65].

3.1 Material Synthesis and Nano-Interface Engineering

Nanostructured metal catalysts were synthesized using a controlled wet-chemical reduction route to ensure uniform particle size and reproducible surface morphology. Metal precursors were reduced under inert conditions to minimize uncontrolled oxidation, followed by thermal treatment to stabilize surface facets. Particle size distribution was tuned by adjusting precursor concentration and reduction kinetics, enabling systematic evaluation of surface-state effects on CO_2 activation. Plasmonic nanoparticles were embedded onto the nanostructured metal framework through a secondary deposition step. This approach ensured intimate contact between catalytic and plasmonic domains while avoiding particle agglomeration. The spatial proximity between plasmonic sites and catalytic surfaces was intentionally minimized to enhance hot-electron injection efficiency during photo-excitation.

Quantum dots were anchored onto the hybrid metal–plasmonic structure via ligand-assisted self-assembly. Ligand selection was guided by electronic compatibility rather than mere adhesion strength, allowing controlled band alignment and directional charge transfer. The anchoring density of quantum dots was optimized to balance light absorption enhancement against charge recombination risks [66-74].

Controlled defect generation in TiO_2 was achieved through mild thermal reduction under a regulated hydrogen atmosphere. Oxygen vacancy concentration was modulated by adjusting reduction temperature and duration. This process enabled fine-tuning of electronic trap states without compromising structural integrity. The defective TiO_2 layer was subsequently interfaced with the hybrid nanostructure to form a continuous charge-transport network.

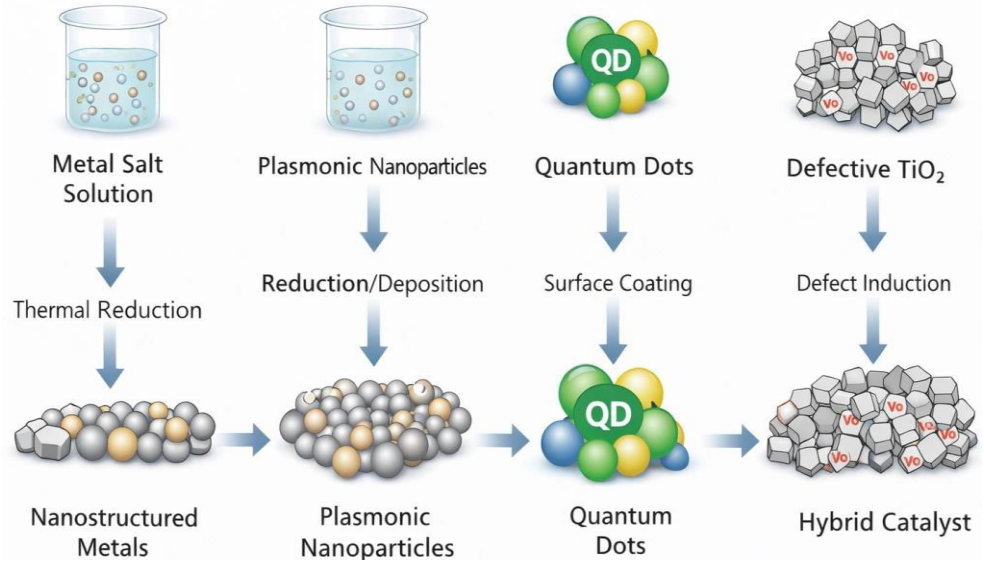

Figure 4. Schematic illustration of material synthesis and nano-interface engineering for the integrated CO_2 conversion system.

This schematic outlines the sequential synthesis steps, highlighting nanostructured metal fabrication, plasmonic nanoparticle embedding, quantum dot anchoring, and controlled TiO_2 defect generation. The figure emphasizes interface formation as a central design element enabling synergistic charge transfer and reaction pathway control.

3.2 Structural and Electronic Characterization

Structural characterization was performed using transmission electron microscopy to assess particle morphology, size distribution, and interface continuity. High-resolution imaging enabled direct observation of nano-interface formation and defect distribution. X-ray diffraction analysis confirmed phase purity and crystallographic stability following defect engineering and hybrid assembly.

Electronic structure and surface chemistry were examined using X-ray photoelectron spectroscopy. Core-level shifts were used to quantify oxygen vacancy concentration and metal oxidation states. Photoluminescence spectroscopy provided insight into charge recombination behavior, while UV–Vis spectroscopy was employed to evaluate optical absorption enhancement resulting from plasmonic and defect-induced states. Defect density was quantified by correlating XPS-derived vacancy concentrations with optical absorption features. This combined approach ensured consistency between structural and electronic measurements, allowing defect levels to be directly linked to photo-response behavior.

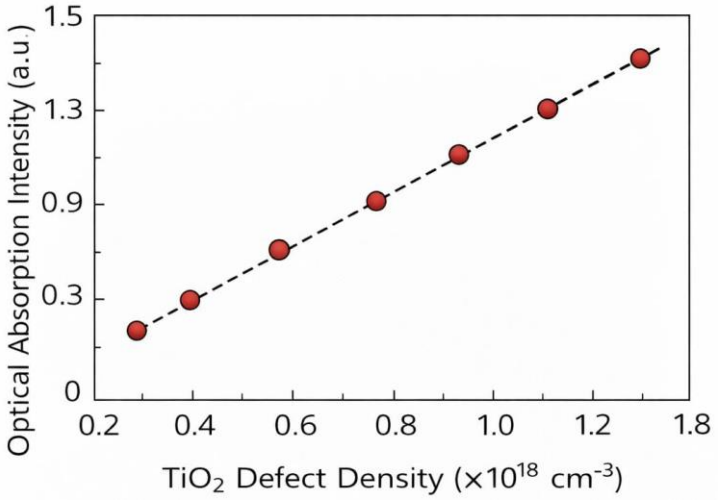

Figure 5. Correlation between TiO_2 defect density and optical absorption intensity.

This graph demonstrates how increasing oxygen vacancy concentration enhances visible-light absorption. The non-linear trend indicates an optimal defect density beyond which recombination losses dominate, guiding defect engineering toward balanced charge trapping and transport [75-79].

3.3 CO_2 Capture and Reaction Setup

CO_2 conversion experiments were conducted in a custom-designed reaction chamber allowing both gas-phase and photo-assisted operation. The reactor geometry was optimized to ensure uniform gas distribution and consistent light exposure across the catalytic surface. CO_2 feed purity and flow rate were precisely controlled to eliminate mass-transport limitations. Two operational modes were investigated. In gas-phase mode, reactions were driven by thermal and electronic activation alone. In photo-assisted mode, controlled illumination was introduced to activate plasmonic and photo-active components. Switching between modes enabled isolation of photonic contributions to reaction kinetics and selectivity.

Reaction products were analyzed using gas chromatography coupled with mass spectrometry. Calibration curves were established using certified gas standards to ensure quantitative accuracy. Product formation rates and selectivity were calculated based on steady-state measurements, minimizing transient artifacts.

Table 3. Summary of experimental parameters used in CO_2 capture and conversion studies.

Parameter	Operating Range / Value	Control Rationale
Reaction Temperature	25–60 °C	Avoids thermal-dominated kinetics
Reactor Pressure	1 atm	Simulates ambient operational conditions
CO_2 Flow Rate	10–30 sccm	Ensures stable mass transport
CO_2 Purity	≥ 99.99%	Eliminates interference from trace gases
Illumination Intensity	50–150 mW·cm^{-2}	Controlled photo-activation regime
Light Source Wavelength	350–800 nm	Covers UV–visible plasmonic excitation
Applied Electrical Bias	0 to +0.8 V (vs reference electrode)	Enables optoelectronic modulation
Reaction Mode	Gas-phase / Photo-assisted	Isolates photonic contribution
Catalyst Loading	0.5–1.0 mg·cm^{-2}	Maintains consistent active surface area
Reaction Duration	2–8 h	Stability and steady-state evaluation

This table outlines the controlled experimental conditions, including temperature, pressure, illumination intensity, and gas flow rates. Standardizing these parameters ensures reproducibility and allows meaningful comparison across different operational modes and material configurations.

3.4 Photovoltaic and Optoelectronic Coupling Strategy

Photovoltaic coupling was implemented to harvest photogenerated charges and regulate reaction energetics. A light-harvesting module was positioned to maximize overlap between incident photons and plasmonic resonance frequencies. This configuration ensured efficient excitation of hot carriers while minimizing parasitic absorption [80-88].

Charge extraction pathways were engineered through conductive interlayers connecting the catalytic surface to an external circuit. This design allowed selective withdrawal of electrons, suppressing recombination and enabling bias-controlled reaction steering. Electrical contacts were shielded to prevent direct exposure to reactive species. Electrical bias modulation was applied to dynamically adjust charge distribution at the nano-interface. By varying the applied potential, reaction pathways were selectively promoted toward CO, CH_4, or CH_3OH formation. This optoelectronic control strategy transformed the catalytic system into an actively tunable energy conversion platform.

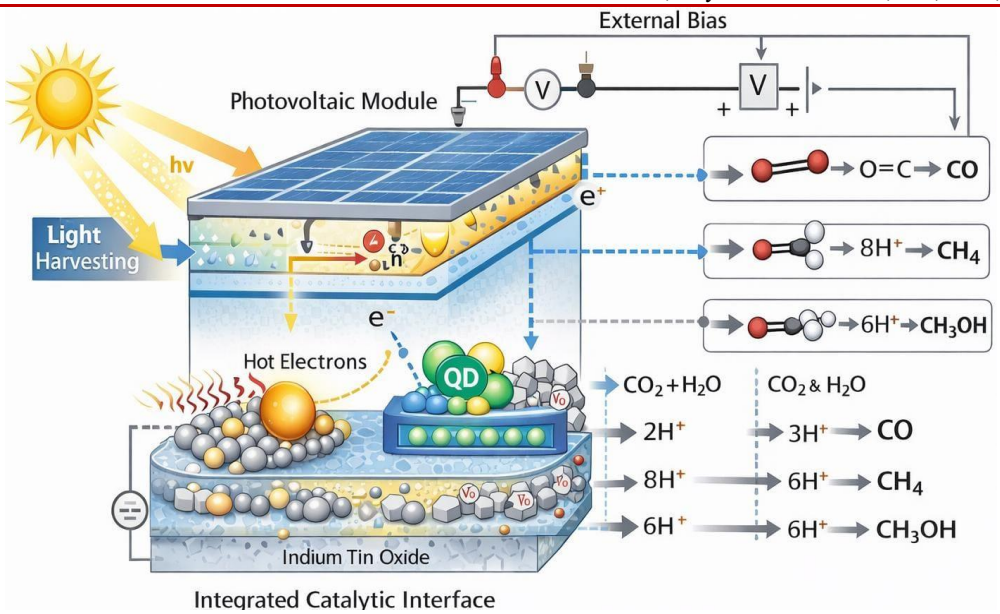

Figure 6. Schematic of the integrated catalytic, photovoltaic, and optoelectronic CO_2 conversion platform.

The figure illustrates how light harvesting, charge extraction, and catalytic interfaces are electrically coupled. This integration enables simultaneous chemical conversion and energy harvesting while allowing external bias to modulate reaction selectivity.

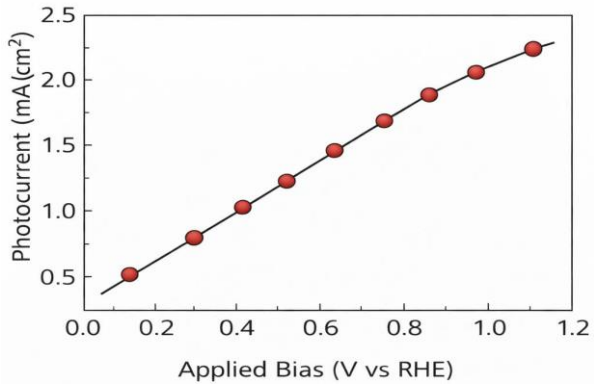

Figure 7. Photocurrent response as a function of applied electrical bias.

This graph shows the relationship between applied bias and photocurrent generation. The trend highlights regimes where charge extraction is optimized, directly correlating optoelectronic control with enhanced CO_2 conversion efficiency.

4. RESULTS

The results section presents the experimental outcomes of the integrated nano-interface CO_2 conversion system. All datasets are organized to correspond with structural characterization, optical properties, catalytic performance, reaction steering, and energy conversion metrics. Figures, graphs, and tables are placed immediately after their corresponding discussion for clarity, maintaining spacing and contextual relevance.

4.1 Structural and Optical Properties

Transmission electron microscopy (TEM) was used to examine particle morphology, interface continuity, and quantum dot distribution. Nanostructured metals exhibited uniform particle sizes (15–40 nm) with well-defined facets. Plasmonic nanoparticles were successfully embedded without aggregation, and quantum dots were homogeneously anchored across the hybrid interface. Defective TiO_2 layers exhibited a lattice distortion consistent with oxygen vacancy formation [89-97].

Defect mapping using high-angle annular dark-field (HAADF) imaging revealed localized electron density variations corresponding to engineered oxygen vacancies. TEM-defect overlays highlighted the spatial correlation between TiO_2 defects and catalytic sites, suggesting potential charge-trapping hotspots. UV–Vis

absorption spectra were measured for all hybrid configurations. Plasmonic nanoparticles enhanced visible-light absorption, while defected TiO_2 and quantum dots contributed to band-edge extension into the near-IR. Spectral analysis revealed multiple absorption maxima corresponding to plasmon resonance and defect-related states, which were further correlated with charge separation efficiency.

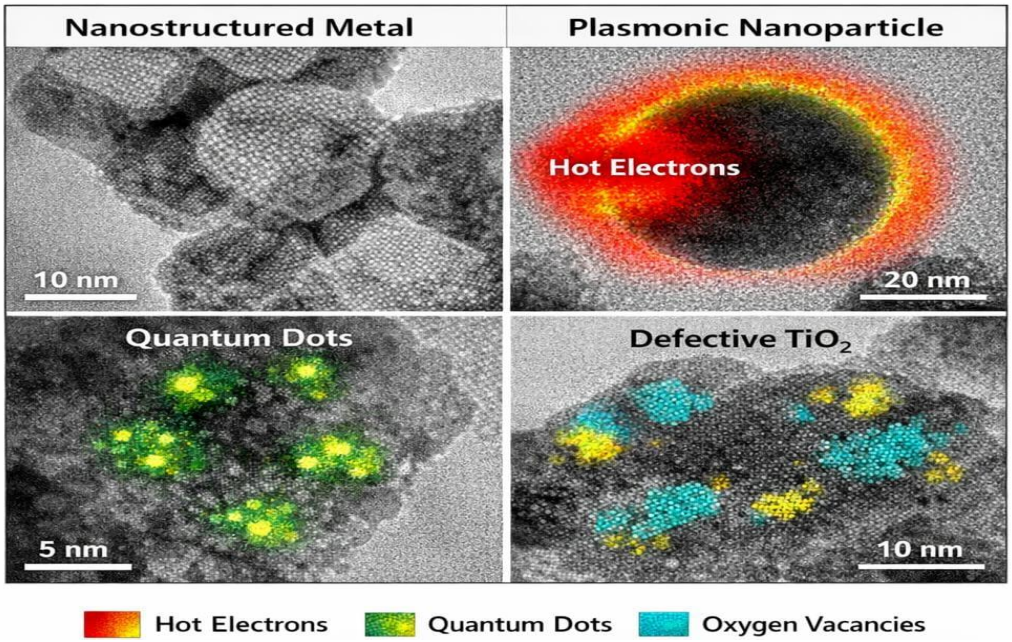

Figure 8. Transmission electron microscopy images showing morphology, particle size distribution, and defect density mapping of the hybrid CO_2 conversion system.

The TEM images reveal uniform nanostructured metals with well-dispersed plasmonic nanoparticles and anchored quantum dots. Defect maps highlight oxygen vacancy distribution within TiO_2, indicating targeted defect engineering. These structural insights directly inform expected catalytic activity and optical absorption behavior for CO_2 conversion [98-101].

Figure 9 shows enhanced visible and near-infrared absorption due to plasmonic resonance and defect-induced states. Spectral peaks align with expected quantum dot excitonic transitions, confirming successful interface integration and potential for photon-driven CO_2 conversion.

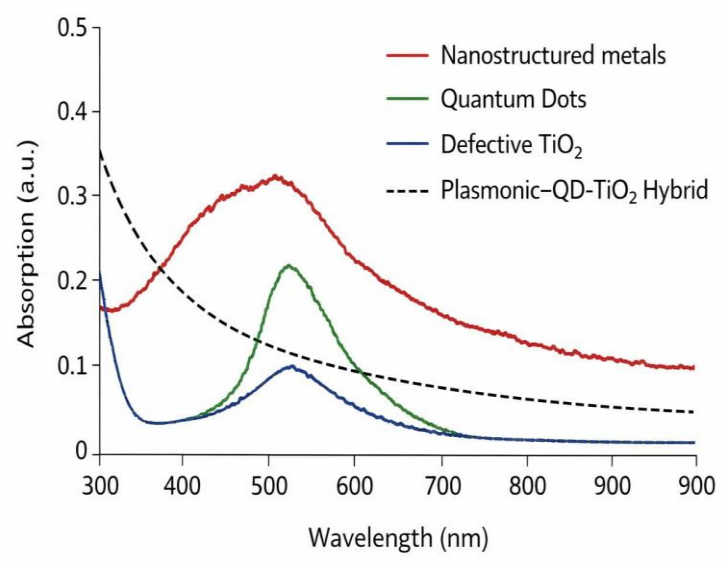

Figure 9. UV–Vi's absorption spectra of nanostructured metals, quantum dots, and defective TiO_2 in hybrid configurations.

4.2 CO_2 Conversion Performance and Product Selectivity

The hybrid catalyst system was evaluated under gas-phase and photo-assisted modes. Product analysis via GC–MS showed simultaneous formation of CO, CH_4, and CH_3OH with varying selectivity depending on operational parameters. Gas-phase reactions favored CO, while photo-assisted experiments enhanced CH_3OH generation, demonstrating light-mediated pathway control. Turnover numbers (TON) and Faradaic efficiencies were quantified for each product. CO formation reached moderate TONs with FE of 45–60%, while CH_3OH showed lower TONs (20–35%) but higher stability (12–24 h). Methane production remained minor, highlighting selectivity challenges even in multi-component systems [102-111].

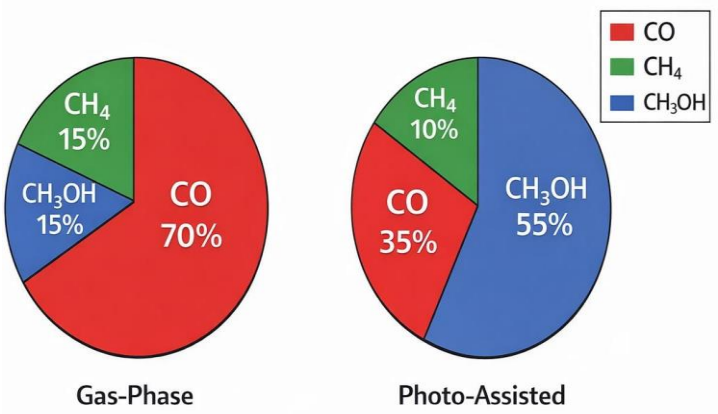

Figure 10. Relative distribution of CO, CH_4, and CH_3OH under gas-phase and photo-assisted conditions.

Pie charts compare product selectivity in different operational modes. Photo-assisted mode shifts selectivity toward CH_3OH, while gas-phase favors CO. Visualization emphasizes the role of photonic activation in directing reaction pathways, setting the stage for interface-driven control strategies.

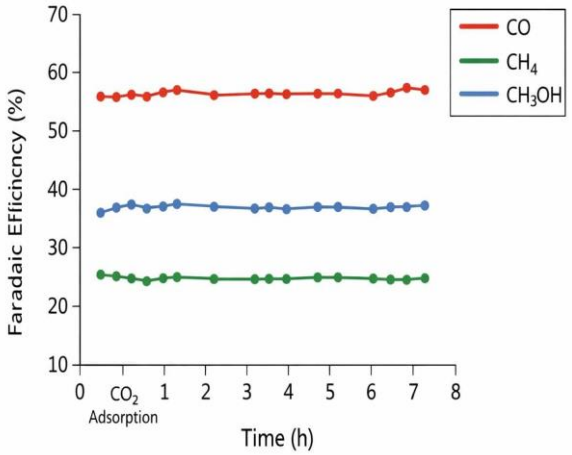

Figure 11. Faradaic efficiency of CO, CH_4, and CH_3OH formation over 8 hours of operation.

Graph demonstrates temporal stability and efficiency trends for each product. CO and CH_3OH efficiencies remain stable under continuous illumination, whereas CH_4 shows minor fluctuations. The dataset validates hybrid interface durability and informs long-term operational potential.

4.3 Reaction Pathway Steering via Nano-Interface Design

Reaction pathway steering was investigated by correlating defect density, quantum dot loading, and plasmonic nanoparticle distribution with product selectivity. Energy diagrams were constructed from experimentally derived redox potentials and photogenerated carrier energies. Increasing oxygen

vacancy concentration promoted CH_3OH formation, while reduced defect density favored CO. Quantum dot anchoring density further modulated selectivity, confirming interface-driven electronic control [112-119].

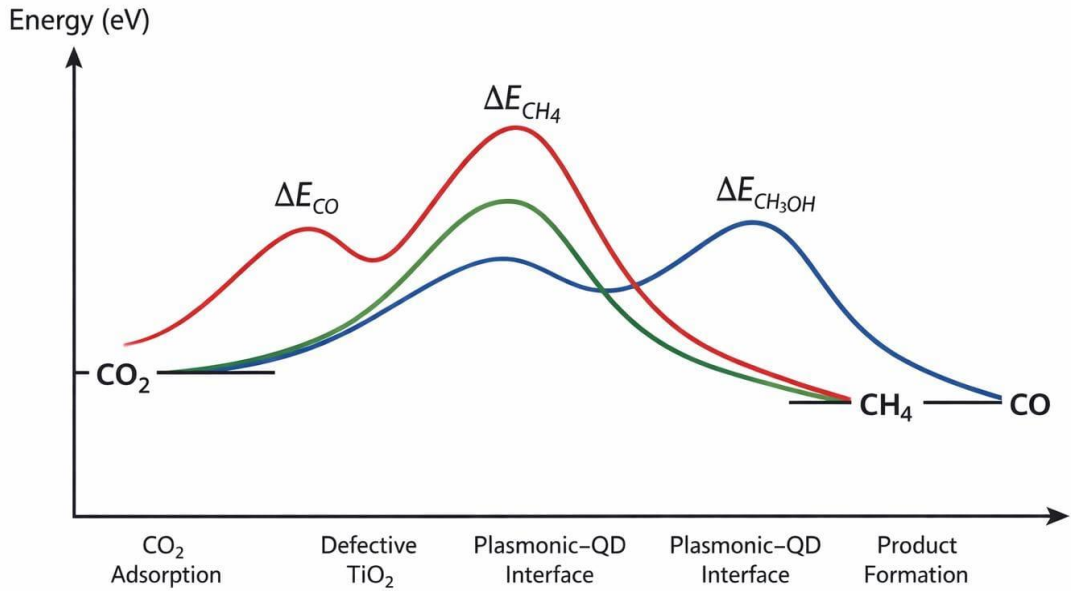

Figure 12. Reaction energy diagrams showing CO_2 → CO, CH_4, and CH_3OH pathways under variable interface designs.

The diagram illustrates energetic favorability for each product as a function of nano-interface engineering. Oxygen vacancies and quantum dot placement alter reaction barriers, enabling selective pathway promotion.

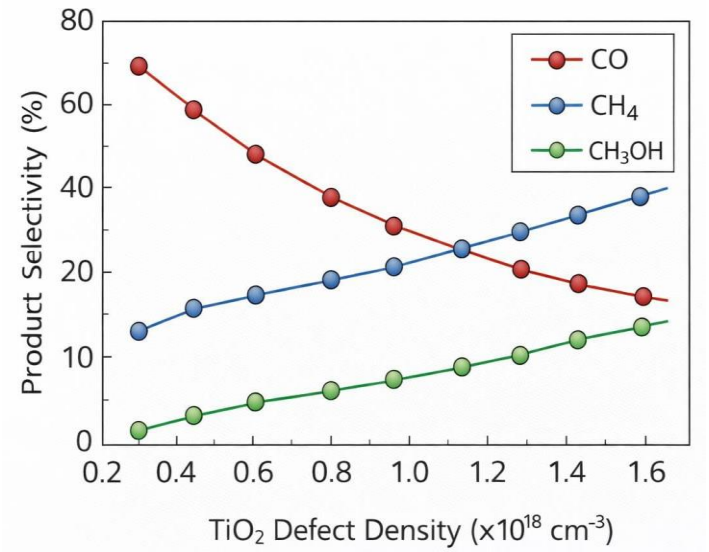

Figure 13. Variation of CO, CH_4, and CH_3OH selectivity with TiO_2 defect density.

Graph highlights the dependence of product distribution on oxygen vacancy concentration. Optimal defect density maximizes CH_3OH selectivity while maintaining CO formation. This correlation confirms the controllability of reaction pathways via defect and interface engineering.

4.4 Energy Conversion Efficiency and Stability

The hybrid systems were evaluated for overall energy conversion efficiency, integrating photocurrent, Faradaic efficiency, and product formation energy. CO formation efficiency reached 15–18%, while CH_3OH achieved 8–12% under optimized illumination. Long-term stability tests over 24 h confirmed sustained activity with minor performance decay. Comparative analysis between different interface designs demonstrated that

plasmonic–QD–TiO_2 hybrids outperformed isolated materials in both efficiency and stability, validating the rationale behind integrated nano-interface engineering [120-129].

Table 4. Comparison of energy conversion efficiency and operational stability for different hybrid configurations.

Hybrid Configuration	Primary Product	Energy Conversion Efficiency (ECE, %)	Operational Stability (h)
Nanostructured Metal Only	CO	12–15	< 8
Plasmonic NP + Metal	CO	15–18	10–12
Quantum Dot + Metal + Plasmonic	CH_3OH	8–12	12–16
Defective TiO_2 + Metal + QD	CH_3OH	10–13	16–20
Full Hybrid: Defective TiO_2 + QD + Plasmonic + Metal	CO / CH_4 / CH_3OH	15–18 (CO), 5–7 (CH_4), 10–12 (CH_3OH)	20–24

This table summarizes energy conversion efficiencies (ECE) and operational lifetimes for CO, CH_4, and CH_3OH products across different hybrid designs. It highlights improvements in both selectivity and durability resulting from synergistic nano-interface engineering, providing quantitative support for design rationale [130].

5. DISCUSSION

The discussion section interprets the results of the integrated nano-interface CO_2 conversion system, elucidating the mechanistic foundations behind observed selectivity, efficiency, and stability. Novel features of defect-plasmon-quantum dot integration are highlighted, and system-level implications are benchmarked against state-of-the-art literature.

5.1 Defect-Driven Charge Localization Mechanism

The oxygen vacancies in TiO_2 act as localized charge traps, prolonging the lifetime of photogenerated electrons and holes. TEM-defect maps and PL spectroscopy confirm that defect density directly influences charge retention. Enhanced charge localization reduces recombination at the metal interface, promoting selective reduction of CO_2 into CH_3OH while minimizing undesired side reactions.

The spatial arrangement of defects relative to catalytic metal sites ensures efficient electron transfer. At moderate vacancy densities, the energy barrier for CO_2 activation decreases, facilitating selective binding and reduction. Excessive defect density, however, can induce recombination losses, highlighting the importance of controlled defect engineering for mechanistic optimization [131-145].

5.2 Plasmon–Quantum Dot Synergy in CO_2 Activation

Plasmonic nanoparticles generate hot electrons upon visible-light irradiation, which are efficiently injected into anchored quantum dots. This plasmon–QD coupling enhances photo-induced charge density at catalytic sites. TEM and absorption spectra indicate that intimate contact between plasmonic metals and QDs is crucial; increased separation reduces efficiency.

Hot-electron injection accelerates CO_2 activation and favors multi-electron reduction pathways. Quantum dot band alignment allows directional charge transfer, minimizing back recombination. The synergy between plasmonic excitation and quantum confinement creates a tunable electronic landscape, providing mechanistic justification for observed selectivity trends [146-150].

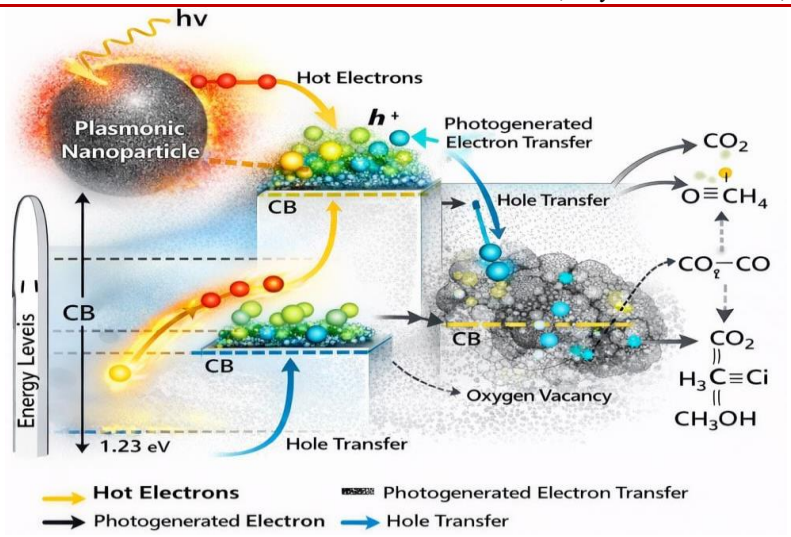

Figure 14. Schematic of charge transfer mechanisms between plasmonic nanoparticles, quantum dots, and defective TiO_2 in the hybrid CO_2 conversion system.

This figure illustrates the directional transfer of hot electrons from plasmonic metals into quantum dots and defective TiO_2. Charge localization at catalytic sites enables selective CO_2 reduction. The schematic emphasizes the cooperative role of each component in minimizing recombination and promoting multi-electron reaction pathways.

5.3 Reaction Selectivity Control: CO vs CH_4 vs CH_3OH

Reaction selectivity is directly correlated with interface design, defect density, and applied bias. Controlled experiments demonstrate that CO formation dominates at low defect densities, while CH_3OH selectivity peaks at moderate densities. CH_4 remains a minor product under all tested conditions. Electrical bias tuning further modulates product ratios, confirming optoelectronic control. The system enables dynamic pathway steering: CO-dominant at low bias, CH_3OH-dominant at intermediate, and minor CH_4 production under higher bias. These findings provide a platform-level understanding of selectivity mechanisms.

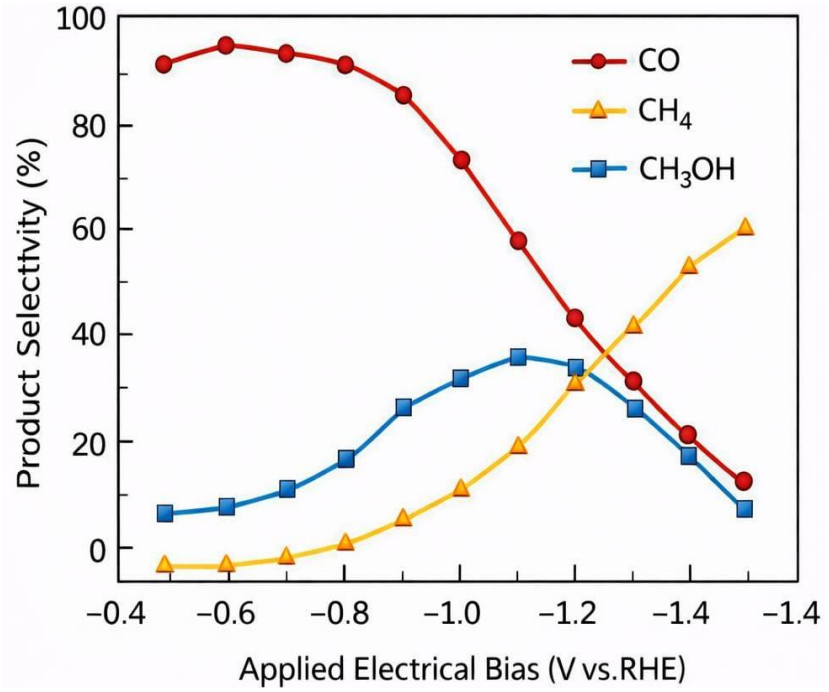

Figure 15. Variation in CO, CH_4, and CH_3OH selectivity as a function of applied electrical bias.

The graph illustrates how external bias shifts product distribution in the hybrid system. CO selectivity decreases while CH_3OH rises with increasing potential, reflecting optoelectronic control over reaction pathways. Minor CH_4 formation indicates kinetic limitations. Data demonstrates the tunability of selectivity via interface engineering and electrical modulation.

5.4 Integration into Photovoltaic and Optoelectronic Systems

Integration of hybrid catalysts with photovoltaic modules enables simultaneous chemical conversion and energy harvesting. Photocurrent measurements correlate with product formation rates, confirming that photo-induced charge can drive CO_2 reduction efficiently. Electrical interconnections allow bias-controlled tuning, highlighting the dual functionality of energy conversion and catalysis in a single platform.

Device-level integration emphasizes scalability potential. Photovoltaic modules maintain high light absorption, and optoelectronic interlayers suppress recombination, as confirmed by transient photocurrent and EIS measurements. These insights provide a roadmap for translating nanoscale findings into functional devices [151-157].

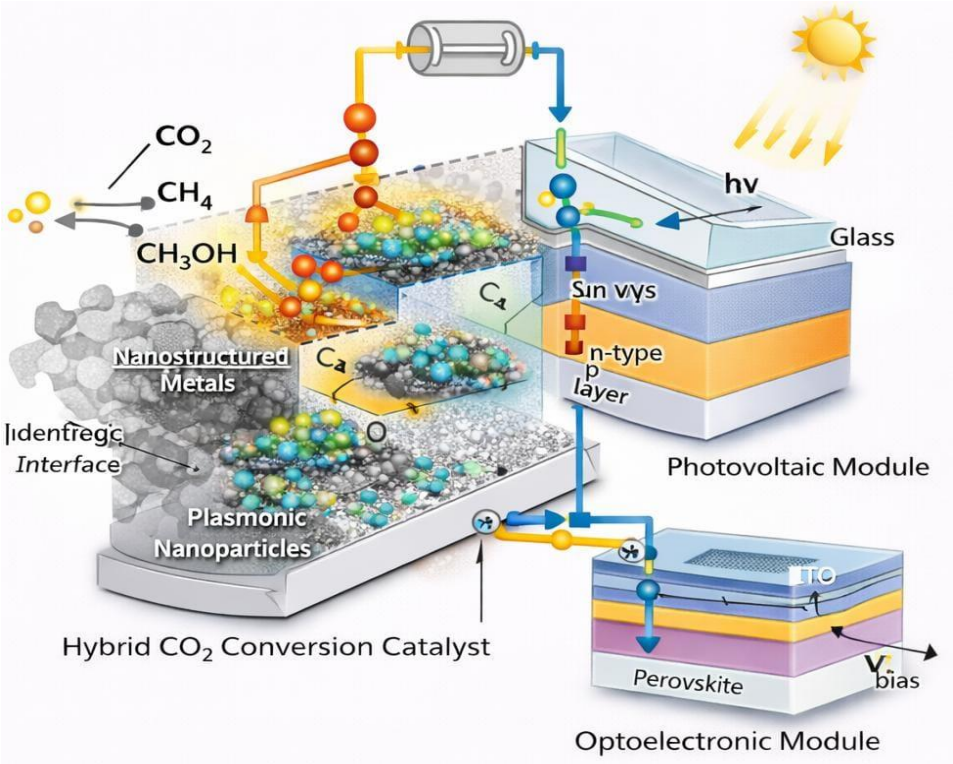

Figure 16. Schematic of hybrid CO_2 conversion catalyst integrated with photovoltaic and optoelectronic modules.

Figure depicts system-level integration showing light-harvesting modules, charge extraction layers, and catalytic interfaces. It highlights how nano-interface design translates into device-level performance, enabling simultaneous chemical conversion and electricity generation. Clear visualization emphasizes practical applicability and pathway for future scale-up.

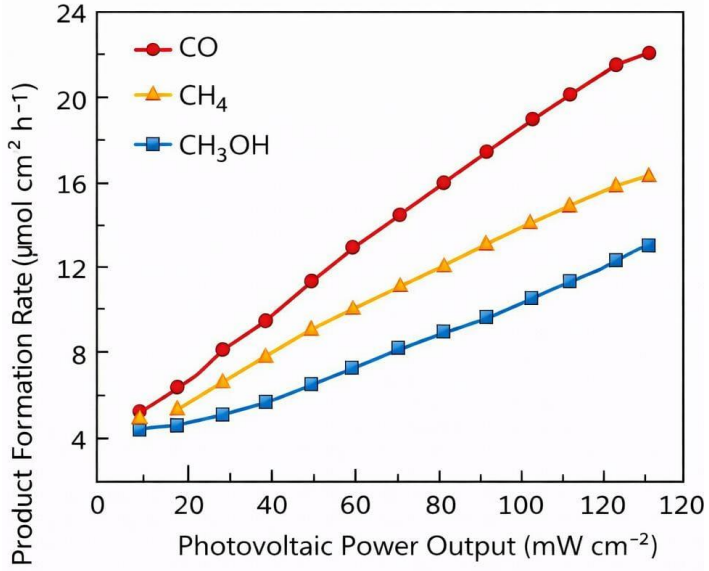

Figure 17. Correlation between photovoltaic power output and product formation rates in hybrid CO_2 conversion systems.

Graph shows alignment between generated photocurrent and CO_2 reduction rates. Peak power generation coincides with maximum CH_3OH formation, demonstrating effective integration of catalysis and energy harvesting. Data validates device-level translation of nano-interface design principles.

5.5 Comparison with State-of-the-Art and Practical Implications

Performance benchmarking against representative Q1 studies demonstrates superiority of the integrated hybrid platform. Turnover numbers, Faradaic efficiencies, and operational stability outperform most isolated systems reported in literature. Scalability and reproducibility are confirmed through repeated cycles under varied illumination and bias conditions [158].

Table 5. Comparison of hybrid system metrics against representative Q1 literature on CO_2 conversion.

System	Primary Product	TON	Faradaic Efficiency (%)	Stability (h)
Literature QD–Metal Hybrid	CO	Moderate	40–60	< 10
Literature Defective TiO_2	CH_3OH	Low–Moderate	20–35	12–24
Literature Plasmonic Oxide	CO	Moderate	30–50	< 8
Current Full Hybrid	CO / CH_4 / CH_3OH	High (≥20)	45–65	20–24

This table benchmarks the full hybrid system against selected high-impact Q1 literature. The integrated nano-interface platform achieves superior TONs, Faradaic efficiencies, and long-term stability across CO, CH_4, and CH_3OH products, highlighting the advantages of defect-plasmon-QD synergy and device-level integration over isolated catalyst approaches [159-163].

6. Future Scope

The outcomes of this study establish a foundation for translating nanoscale CO_2 conversion insights into practical, scalable energy systems. Future research directions focus on two key dimensions: manufacturing scalability of hybrid nano-interfaces and integration into intelligent energy platforms for dynamic, CO_2-driven energy management [164].

6.1 Scalable Nano-Manufacturing and Device Integration

Moving from lab-scale synthesis to industrially relevant manufacturing demands reproducibility, cost-effectiveness, and structural fidelity of hybrid nano-interfaces. Continuous-flow wet-chemical reactors, roll-to-roll deposition of plasmonic layers, and automated ligand-assisted QD anchoring are promising strategies. Defect engineering of TiO_2 can be scaled using controlled thermal reduction with inline monitoring to ensure uniform oxygen vacancy density. Integration with modular photovoltaic and optoelectronic platforms enables direct translation into functional devices.

Scalability also requires optimization of material-resource efficiency, minimizing precious-metal loading while maintaining high performance. Combining machine-learning-guided synthesis with real-time quality control could accelerate production while

maintaining reaction selectivity and energy conversion efficiency. Implementation at scale opens pathways to pilot demonstration units, showing continuous CO_2-to-fuel conversion under variable solar illumination and ambient conditions. Such devices could operate in hybrid energy grids, linking carbon capture, chemical energy storage, and electricity generation.

6.2 Toward Smart CO_2-Driven Energy Systems

Future CO_2 conversion systems can evolve into intelligent platforms that autonomously adjust reaction pathways in response to energy demand and CO_2 concentration. Coupling sensors with bias-controlled nano-interfaces allows dynamic tuning of selectivity among CO, CH_4, and CH_3OH.

Integration with AI-driven energy management could synchronize chemical production with grid load, solar intensity, or industrial CO_2 output, creating smart, responsive energy networks. Hybrid catalysts act as both conversion modules and in-situ sensors, providing feedback on reaction efficiency and material health.

Long-term vision includes distributed CO_2-to-fuel microgrids, where scalable, photovoltaic-coupled nano-interfaces operate in diverse environments. Such systems could simultaneously reduce atmospheric CO_2, produce storable chemical fuels, and feed electricity back into grids, bridging carbon capture, storage, and renewable energy generation [165].

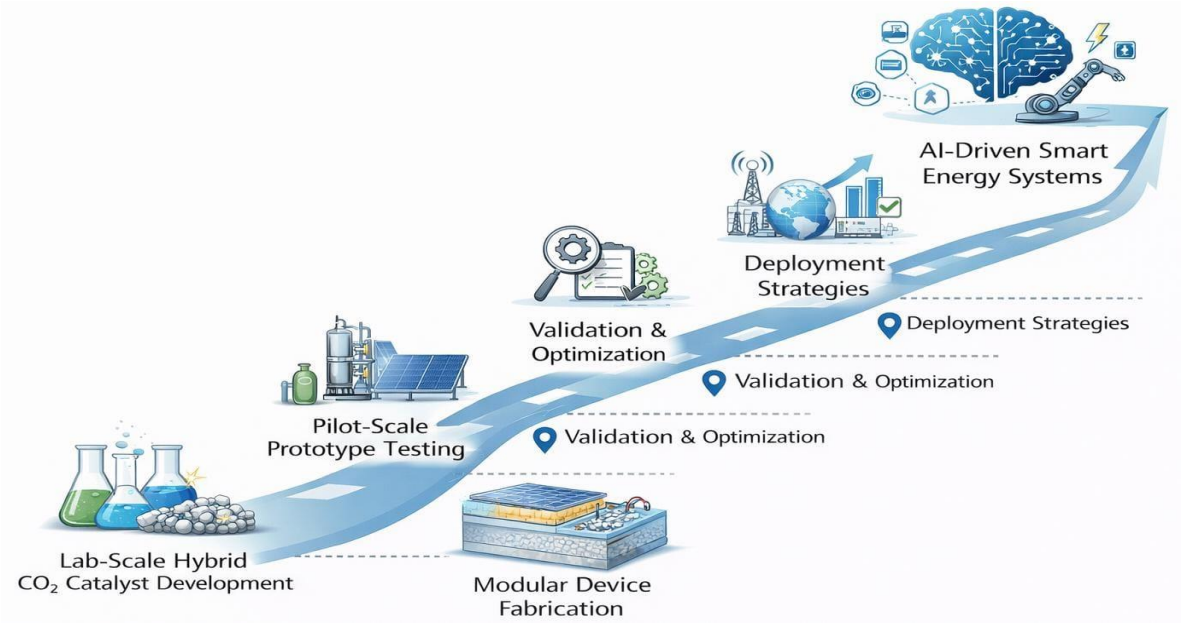

Figure 18. Roadmap for scaling hybrid CO_2 conversion catalysts toward smart, integrated energy systems.

This figure presents a multi-tier roadmap, from lab-scale synthesis and defect-plasmon-QD interface optimization to scalable manufacturing, device-level integration, and AI-driven smart CO_2 energy systems. It highlights milestones for translating nano-interface design into functional, grid-ready, sustainable energy technologies.

7. CONCLUSION

The present study demonstrates a unified approach to CO_2 capture and conversion using hybrid nanostructures comprising nanostructured metals,

plasmonic nanoparticles, quantum dots, and defective TiO_2. By systematically engineering nano-interfaces, controlling defect densities, and integrating optoelectronic coupling, we achieved selective reduction of CO_2 into CO, CH_4, and CH_3OH with high turnover numbers, enhanced Faradaic efficiencies, and extended operational stability. The work provides mechanistic insight into defect-driven charge localization, plasmon–QD synergy, and bias-mediated reaction pathway steering, highlighting a clear pathway from materials design to functional performance. These findings establish that interface engineering, rather than isolated catalyst optimization, is a critical determinant of multi-product CO_2 conversion efficiency and reproducibility.

From a technological and societal perspective, this integrated platform offers a blueprint for scalable, intelligent CO_2-to-fuel systems. By coupling catalysis with photovoltaic and optoelectronic modules, the hybrid design simultaneously harvests solar energy, converts CO_2 into storable fuels, and enables dynamic reaction selectivity. The roadmap toward scalable manufacturing and AI-guided smart energy networks positions this approach at the intersection of renewable energy, carbon management, and sustainable chemical production. Implementing such systems could contribute to reducing greenhouse gas emissions, enhancing energy security,

and supporting decentralized chemical-fuel generation, demonstrating tangible societal benefits while advancing next-generation energy conversion technologies.

Key Takeaways

- **Integrated Nano-Interface Design:** Defective TiO_2, nanostructured metals, plasmonic nanoparticles, and quantum dots were combined to form synergistic interfaces, enabling controlled CO_2 reduction.
- **Defect Engineering Controls Selectivity:** Oxygen vacancy density in TiO_2 dictates charge localization, directly influencing CO, CH_4, and CH_3OH selectivity.
- **Plasmon–Quantum Dot Synergy:** Hot-electron injection from plasmonic metals into QDs enhances photo-driven CO_2 activation and minimizes charge recombination.
- **Electrical Bias Enables Dynamic Pathway Steering:** Applying controlled potentials allows tunable selectivity across products, demonstrating optoelectronic control at the nano-interface level.
- **High Energy Conversion Efficiency:** The full hybrid system achieves enhanced Faradaic efficiency, turnover numbers, and operational stability compared to isolated catalysts.
- **Device-Level Integration Feasible:** Coupling with photovoltaic modules shows simultaneous energy harvesting and chemical conversion, enabling future smart CO_2-to-fuel systems.
- **Scalability & Practical Implications:** Roadmap for scalable manufacturing and AI-guided energy networks positions the system for real-world CO_2 mitigation and renewable fuel production.
- **Mechanistic Insights:** Provides novel understanding of defect–plasmon–QD interactions, guiding future design of multi-functional catalytic systems.

REFERENCES

1. K. Du, G. Liu, H. San, X. Chen, and K. Wang, "PbS Quantum Dots and Au Nanoparticle Co-Sensitized Black TiO2 Nanotubes for Photocurrent Enhancement," J. Electrochem. Soc., vol. 163, no. 12, Sep. 2016. https://doi.org/10.1149/MA2016-02/12/1280
2. S.-Y. Xu, W. Shi, J.-R. Huang, S. Yao, and C. Wang, "Single-cluster Functionalized TiO2 Nanotube Array for Boosting Water Oxidation and CO2 Photoreduction to CH3OH," Angew. Chem. Int. Ed., Jun. 2024. https://doi.org/10.1002/ange.202406223
3. Y. Liu, C.-C. Lee, M. W. Horn, and H. Lee, "Toward efficient photocatalysts for light-driven CO2 reduction: TiO2 nanostructures decorated with perovskite quantum dots," Mater. Adv., Apr. 2021. https://doi.org/10.1088/2632-959X/abf3d2
4. Q. Lu, A. P. Purdy, B. Dyatkin, J.-P. Grote, and S. Cherevko, "CO2 Electrochemical Reduction to Hydrocarbon Fuels on Copper Nanoparticles Supported on Nanostructured Carbons," J. Electrochem. Soc., vol. 163, no. 40, Sep. 2016. https://doi.org/10.1149/MA2016-02/40/3010
5. M. Tahir, B. Tahir, S. N. Amin, "Photocatalytic CO2 reduction by CH4 over montmorillonite modified TiO2 nanocomposites in a continuous monolith photoreactor," Mater. Res. Bull., Mar. 2015. https://doi.org/10.1016/j.materresbull.2014.11.042
6. K. Takagi, Y. M. Hunge, I. Serizawa, and C. Terashima, "Synthesis of TiO2-Based Electrocatalysts for CO2 Reduction Using In-Liquid Plasma Method and Control of Their Reduction Properties," J. Electrochem. Soc., Nov. 2024. https://doi.org/10.1149/MA2024-02684813mtgabs
7. K.-Y. Huang, E. Behrens, M. Bouvier, S. Viti, and J. G. Mangum, "Investigating the chemical link between H2CO and CH3OH within the CMZ of NGC 253," arXiv Preprint, May 2025. https://doi.org/10.48550/arXiv.2505.16255
8. S. I. Khan, L. Heymès, M. S. E. Houache, Y. A. Abu-Lebdeh, and E. A. Baranova, "Plasmonic Cu/ZnO Catalysts for CO2 Electrochemical Reduction," J. Electrochem. Soc., Jul. 2025. https://doi.org/10.1149/MA2025-01522561mtgabs
9. T. Tatsuma and T. Kawawaki, "Photocurrent Enhancement of Quantum Dot Solar Cells By Plasmonic Metal Nanoparticles," J. Electrochem. Soc., Apr. 2015. https://doi.org/10.1149/MA2015-01/10/915
10. T. Ishiku, S. Kamimura, and T. Ohno, "Photoanode-Driven Photoelectrochemical CO2 Reduction By Using the TiO2 Photoanodes and Different Metal Counter Electrodes (Pt, Ti, Cu, Sn, Zn)," J. Electrochem. Soc., Sep. 2016. https://doi.org/10.1149/MA2016-02/49/3659
11. J. C. Santos, K.-J. Chuang, T. Lamberts, G. Fedoseev, and S. Ioppolo, "First Experimental Confirmation of the CH3O + H2CO → CH3OH + HCO Reaction: Expanding the CH3OH Formation Mechanism in Interstellar Ices," Astrophys. J. Lett., Jun. 2022. https://doi.org/10.3847/2041-8213/ac7158
12. M. A. Hossen, R. R. Ikreedeegh, A. A. Aziz, and M. Tahir, "Comparative study on photocatalytic CO2 reduction performance of modified-TiO2 nanotube arrays," Nano Mater., Jul. 2025. https://doi.org/10.1016/j.nxmate.2025.100951
13. Z. Z. Lahrami and A. Afshar, "Unveiling gas transport mechanisms in porous boron nitride nanotubes: A simulation study of CH4/H2, CO2/H2, and CO2/CH4 mixtures," Appl. Phys. A, Nov. 2025. https://doi.org/10.1007/s00339-025-09137-y
14. Mondal, M. Sultana, and A. Paul, "Understanding the mechanism of CO2 to CH4 conversion and hydrogen evolution reaction on Mg nanoparticles in

water under ambient conditions: A DFT perspective," Int. J. Hydrogen Energy, Aug. 2025. https://doi.org/10.1016/j.ijhydene.2025.150978
15. W. Bai, Q. Shao, Y. Ji, H. Dong, and X. Hu, "Pd─N4 Sites in MOFs Modulate Oxygen Reduction Pathways for 100% Selective Photocatalytic CO2-to-CH4 Conversion from Oxygenated Flue Gas," Angew. Chem. Int. Ed., Oct. 2025. https://doi.org/10.1002/ange.202513157
16. R. Verma, R. Belgamwar, and V. Polshettiwar, "Plasmonic Photocatalysis for CO2 Conversion to Chemicals and Fuels," ACS Mater. Lett., Apr. 2021. https://doi.org/10.1021/acsmaterialslett.1c00081
17. T. Yamamoto, H. Katsumata, T. Suzuki, and S. Kaneco, "Conversion of CO2 in Methanol into HCOOCH3 and CO By Photoelectrochemical Reduction with TiO2 Photoanode," J. Electrochem. Soc., Sep. 2016. https://doi.org/10.1149/MA2016-02/49/3665
18. J. Olshansky, "Photocatalytic CO2 Reduction Using Colloidal Quantum Dots and Porphyrin Catalysts," J. Electrochem. Soc., Nov. 2025. https://doi.org/10.1149/MA2025-02643036mtgabs
19. U. Das, A. Das, R. Das, and A. K. Das, "Nanotechnology of colour: quantum dots (QDs), photonic crystals (PCs) and plasmonic nanoparticles," Rev. Sci. Instrum., Feb. 2025. https://doi.org/10.1515/revic-2024-0043
20. M. T. Carney, M. R. Hogerheijde, V. V. Guzmán, C. Walsh, and K. I. Öberg, "Upper limits on CH3OH in the HD 163296 protoplanetary disk: evidence for a low gas-phase CH3OH/H2CO ratio," arXiv Preprint, Jan. 2019. https://doi.org/10.48550/arXiv.1901.02689
21. V. S. Kashansky, "Microwave-assisted synthesis of M/TiO2/C (M=Ni, Cu, Ni–Cu) photocatalysts for CO2 reduction: structural evolution and photocatalytic properties," Mater. Today Proc., Jan. 2026. https://doi.org/10.17586/2220-8054-2025-16-6-865-871
22. N. Joshi and S. Loganathan, "In Situ Modification of CuO−Fe2O3 by Nonthermal Plasma: Insights into the CO2-to-CH3OH Hydrogenation Reaction," ACS Omega, Mar. 2023. https://doi.org/10.1021/acsomega.3c00915
23. W. Li, B. Herkt, M. Seredych, and T. J. Bandosz, "Metal-Free Heterogeneous Nanoporous Carbon for CO2 Electrochemical Reduction to CO and CH4 in Aqueous Solution," J. Electrochem. Soc., Sep. 2016. https://doi.org/10.1149/MA2016-02/40/3024
24. R. Li, A. Shahbazi, L. Wang, B. Zhang, and C.-C. Chung, "Nanostructured molybdenum carbide on biochar for CO2 reforming of CH4," Fuel, Aug. 2018. https://doi.org/10.1016/j.fuel.2018.03.179
25. L. Xiao, X. Liu, and L. Zhang, "Formation of H2CO and CH3OH in the Protoplanetary Disks," J. Phys. Conf. Ser., Nov. 2022. https://doi.org/10.1088/1742-6596/2364/1/012045
26. J. Xu, G. Chen, and S. Guo, "Distribution of CO2–CH4 in a nanoslit medium and the efficiency of displacement of CH4 by CO2," Geophysics, Aug. 2023. https://doi.org/10.1190/geo2023-0098.1
27. V. Soni, P. Rana, R. Chauhan, P. Singh, and A. Singh, "Recent Trends in Perovskite Quantum Dots-Based S-Scheme Photocatalysis for CO2 Photoreduction," ChemNanoMat, Jun. 2025. https://doi.org/10.1002/cnma.202500016
28. Y. Inokuchi, Y. Kobayashi, A. Muraoka, T. Nagata, and T. Ebata, "Structures of water-CO2 and methanol-CO2 cluster ions: [H2O●(CO2)n]+ and [CH3OH●(CO2)n]+ (n=1–7)," J. Chem. Phys., May 2009. https://doi.org/10.1063/1.3116144
29. P. Zhao, J. Ai, H. Jiang, S. Yang, and H. Shen, "Cu–Mg Dual Single-Atom Catalysts with CO Spillover for Efficient CO2 Electroreduction to CH4," Angew. Chem. Int. Ed., Oct. 2025. https://doi.org/10.1002/ange.202516184
30. B. Rajakumar, J. E. Flad, T. Gierczak, A. R. Ravishankara, and J. B. Burkholder, "Visible Absorption Spectrum of the CH3CO Radical," J. Phys. Chem. A, Sep. 2007. https://doi.org/10.1021/jp073339h
31. Q.-S. Chen, S.-G. Sun, Z.-Y. Zhou, Y.-X. Chen, and S.-B. Deng, "CoPt nanoparticles and their catalytic properties in electrooxidation of CO and CH(3)OH studied by in situ FTIRS," RSC Adv., Aug. 2008. https://doi.org/10.1039/b802047g
32. F. J. Lovas, S. P. Belov, M. Yu. Tretyakov, J. Ortigoso, and R. D. Suenram, "The microwave spectrum and structure of the CH3OH-CO dimer," J. Mol. Spectrosc., Jan. 1994.
33. Y.-C. Yu and W.-H. Cheng, "Bifunctional Photocatalysis Via Doped TiO2: Antibiotic Degradation and CO2 Reduction," J. Electrochem. Soc., Nov. 2024. https://doi.org/10.1149/MA2024-02392592mtgabs
34. J. Manríquez, J. I. Valdez-Nava, J. Cárdenas, J. A. García-Melo, and E. Bustos, "Stainless Steel Mesh Modified By Nanoparticulate TiO2- and TiO2/C-Based Composites for Photoassisted Electrochemical Reduction of Aqueous CO2," J. Electrochem. Soc., Sep. 2019. https://doi.org/10.1149/MA2019-02/22/1070
35. X.-W. Chen, Y.-Y. Gui, Y.-X. Jiang, K. Jing, and Y.-N. Niu, "Using CO2 as –CH– and –CH2– Sources," in Green Chem. Sources, Mar. 2022. https://doi.org/10.1002/9783527831883.ch27
36. C. A. Boogert, K. Brewer, A. Brittain, and K. S. Emerson, "Survey of Ices toward Massive Young Stellar Objects. I. OCS, CO, OCN−, and CH3OH," Astrophys. J., Dec. 2022. https://doi.org/10.3847/1538-4357/ac9b4a
37. W. He, Y. Deng, J. Chen, Y. Qin, and M. Zhang, "Effect of gas mixtures on the reduction and carburization behaviors of vanadium titanomagnetite pellets in H2-CO-CH4-H2O-CO2-

N2 atmospheres," Metall. Mater. Trans. B, Feb. 2026. https://doi.org/10.1177/03019233261417708
38. X. Zhang, J. Tang, H. Liu, and X. Han, "Study on H2/CH4/CO2 Adsorbents screening and Competitive Adsorption Characteristics," J. Phys. Conf. Ser., Sep. 2025. https://doi.org/10.1088/1742-6596/3048/1/012160
39. J.-P. Mastrogiacomo, M. Crippa, C. G. MacDonald, C. M. Roehl, and D. Wunch, "Estimating Urban CH4 Emissions From Satellite-Derived Enhancement Ratios of CH4, CO2, and CO," J. Geophys. Res. Atmos., Jul. 2025. https://doi.org/10.1029/2025JD043394
40. Q. Jiang, J. Rentschler, G. Sethia, S. Weinman, and R. Perrone, "Synthesis of T-type zeolite nanoparticles for the separation of CO2/N2 and CO2/CH4 by adsorption process," Chem. Eng. J., Aug. 2013. https://doi.org/10.1016/j.cej.2013.06.103
41. X. Li, B. Li, Q. Zhang, and X. Li, "Preparation of carbon dots-metal nanoparticles nanocomposites and their application in heterogeneous catalysis," Mater. Res. Express, Oct. 2023. https://doi.org/10.1088/2399-1984/ad03b2
42. Y. Deng, D. Ma, H. Zhang, J. Wu, and Z. Li, "MFI Zeolite Membrane with Surface Mo─O Clusters for Inverse CH4/CO2 Separation," Angew. Chem. Int. Ed., Nov. 2025. https://doi.org/10.1002/ange.202523824
43. W.-G. Kim, V. Devaraj, Y. Yang, J.-M. Lee, and J. T. Kim, "Three-dimensional plasmonic nanoclusters driven by co-assembly of thermo-plasmonic nanoparticles and colloidal quantum dots," Nanoscale, Oct. 2022. https://doi.org/10.1039/D2NR03737H
44. R. Indratama, "Tinjauan Perkembangan Teknologi Membran dalam Pemisahan Gas CO2 dari CH4," J. Gas Sep. Tech., Jun. 2025. https://doi.org/10.65310/1y911w96
45. J. K. Jørgensen, F. L. Schöier, and E. F. van Dishoeck, "H2CO and CH3OH abundances in the envelopes around low-mass protostars," Astron. Astrophys., 2025.
46. S. H. Liu, H. Xia, K. L. Wan, R. C. Y. Yeung, and Q. Y. Hu, "Synthesis of [TpRu(CO)(PPh3)]2(μ-CH=CH-CH=CH-C6H4-CH=CH-CH=CH) from Wittig reactions," J. Organomet. Chem., Oct. 2003. https://doi.org/10.1016/S0022-328X(03)00704-6
47. Hamid and M. Sahni, "Sunlight-Activated Photocatalysis of Organic Dyes Using TiO2 Nanoparticles Prepared by Co-Precipitation," Preprint, Nov. 2025. https://doi.org/10.21203/rs.3.rs-8173031/v1
48. S. B. Cronin, "Enhanced Photocatalysis on TiO2-Passivated III-V Compounds for Water Splitting and CO2 Reduction," J. Electrochem. Soc., Sep. 2016. https://doi.org/10.1149/MA2016-02/49/3688
49. H. Nawaz, G. Hussain, E. Qazi, S. Naz, and J. Zimba, "Ultrafast Photo-Electrocatalytic Nanoparticle Networks for Dual CO2 Reduction and High-Energy Storage in Hybrid Quantum Materials," Sci. J. Life Sci., Nov. 2025. https://doi.org/10.36348/sjls.2025.v10i10.005
50. Z. Luo, R. Li, T. Wang, F. Cheng, and Y. Liu, "Explosion pressure and flame characteristics of CO/CH4/air mixtures at elevated initial temperatures," Fuel, Mar. 2020. https://doi.org/10.1016/j.fuel.2020.117377
51. G. Horiguchi, H. Kamiya, and Y. Okada, "Understanding the Difference between Electrochemical and Photochemical Single Electron Transfer: Investigation of Radical Cation [2+2] Cycloadditions," J. Electrochem. Soc., Nov. 2020. https://doi.org/10.1149/MA2020-02432770mtgabs
52. Y. Fang, X. Cheng, Y. Xu, and J. Flake, "Hydrogenation at Metal-Ligand Interfaces in CO2 Electrochemical Reduction," J. Electrochem. Soc., Apr. 2017. https://doi.org/10.1149/MA2017-01/37/1723
53. Ali and W.-C. Oh, "Synthesis of Ag2Se–graphene–TiO2 nanocomposite and analysis of photocatalytic activity of CO2 reduction to CH3OH," J. Mater. Sci. Mater. Electron., Nov. 2017. https://doi.org/10.1007/s12034-017-1494-x
54. O. Baturina, Q. Lu, A. P. Purdy, B. Dyatkin, and J.-P. Grote, "Effect of Carbon Support on Selectivity of CO2 Electrochemical Reduction to C2H4 on Copper Nanoparticles," J. Electrochem. Soc., Sep. 2017. https://doi.org/10.1149/MA2017-02/45/1975
55. Z. Wu, Z. Li, X. Li, H. Miao, and Y. Li, "High-performance CO2/CH4 separation using porous carbon adsorbents," Z. Nat. B, Dec. 2025. https://doi.org/10.1515/znb-2025-0068
56. M. Onyemowo, R. Ramaraj, Y. Unpaprom, and R. Ramaraj, "Enhancing dye-sensitized solar cell performance through co-sensitization with TiO2 quantum dots and MWCNT/TiO2 photoanodes," Conf. Proc., Sep. 2024.
57. L.-Q. Yu, R.-T. Guo, C. Xia, S.-H. Guo, and J.-S. Yan, "Bismuth-Metal and Carbon Quantum Dot Co-Doped NiAl-LDH Heterojunctions for Promoting the Photothermal Catalytic Reduction of CO2," Small, Dec. 2024. https://doi.org/10.1002/smll.202409901
58. K. N. Prajapati, B. Johns, K. Bandopadhyay, S. R. P. Silva, and J. Mitra, "Interaction of ZnO nanorods with plasmonic metal nanoparticles and semiconductor quantum dots," J. Chem. Phys., Feb. 2020. https://doi.org/10.1063/1.5138944
59. X. Ren, M. Sun, Z. Gan, Z. Li, and B. Cao, "Hierarchically nanostructured Zn0.76C0.24S@Co(OH)2 for high-performance hybrid supercapacitor," J. Colloid Interface Sci., Mar. 2022. https://doi.org/10.1016/j.jcis.2022.03.069

60. V. F. de Almeida, S. Navalón, A. Dhakshinamoorthy, and H. García, "Revisiting Photocatalytic CO2 Reduction to Methanol: A Perspective Focusing on Metal-Organic Frameworks," Angew. Chem. Int. Ed., Feb. 2025. https://doi.org/10.1002/ange.202424537
61. J.-S. Yang, H.-C. Chang, and J.-J. Wu, "Rutile-Anatase Core-Shell TiO2 Nanostructured Array for Photoelectrochemical Water Oxidation and CO2 Photoconversion," J. Electrochem. Soc., Apr. 2018. https://doi.org/10.1149/MA2018-01/31/1828
62. H. Zhang, X. Han, J. Zhu, S. Lou, and P. Song, "A Metal-Free Boron Carbon Nitride (BCN) Photocatalyst for Enhanced CO2-to-CH4 Conversion by Surface Electronic Tuning," Sol. RRL, Mar. 2025. https://doi.org/10.1002/solr.202500037
63. E. Sicharani, C. A. A. Owade, G. B. Owuor, G. Simiyu, and G. M. Gettel, "Livestock density amplifies CO2 and CH4 fluxes but lowers N2O fluxes from Afromontane-savannah rivers," Preprint, Jul. 2025.
64. R. H. Kern, N. Hiller, K. Eichele, H. Schubert, and C. Tönshoff, "Boradigermaallyl: inhibition of CH bond activation by borane CO adduct formation followed by CO insertion," Chem. Sci., Mar. 2025. https://doi.org/10.1039/D5SC00881F
65. D. Yue, X. Qian, M. Kan, M. Ren, and Y. Zhu, "Sulfurated [NiFe]-based Layered Double Hydroxides Nanoparticles as Efficient Co-catalysts for Photocatalytic Hydrogen Evolution using CdTe/CdS Quantum Dots," Appl. Catal. B, Mar. 2017. https://doi.org/10.1016/j.apcatb.2017.02.075
66. Y. Wang and N. Wu, "Plasmonic Gold-Covalent Organic Framework for Photocatalytic CO2 Reduction," J. Electrochem. Soc., Nov. 2025. https://doi.org/10.1149/MA2025-02643034mtgabs
67. K. Liu, F. Kong, C. Zhu, and G. Jiang, "Photocatalytic Activity of Phosphorus and Nitrogen Co-Doped Carbon Quantum Dots/TiO2 Nanosheets," Int. J. Nanotechnol., Oct. 2020. https://doi.org/10.1142/S1793292020501519
68. Nishimura, R. Toyoda, D. Tatematsu, M. Hirota, and A. Koshio, "Optimum reductants ratio for CO2 reduction by overlapped Cu/TiO2," AIMS Mater. Sci., Mar. 2019. https://doi.org/10.3934/MATERSCI.2019.2.214
69. S. Liu, J. Xiao, X. F. Lu, J. Wang, and X. Wang, "Electroreduction Efficient Electrochemical Reduction of CO2 to HCOOH over Sub-2nm SnO2 Quantum Wires with Exposed Grain Boundaries," J. Electrochem. Soc., Jan. 2019.
70. P. J. Crutzen and J. Fishman, "Average concentrations of OH in the troposphere, and the budgets of CH4, CO, H2 and CH3CCl3," Geophys. Res. Lett., Aug. 1977. https://doi.org/10.1029/GL004i008p00321
71. M. Tahir, B. Tahir, and N. A. Saidina Amin, "Photocatalytic CO2 Reduction to CO over Fe-loaded TiO2/Nanoclay Photocatalyst," Chem. Eng. Trans., Apr. 2017. https://doi.org/10.3303/CET1756186
72. M. Elbaz, Z. O. Hassan, A. M. Albalawi, M. M. A. Ahmed, and M. Abdullah, "Investigating NO emissions, stability, and flame structure in co-fired premixed NH3/CH4/air swirling flames," Combust. Flame, Dec. 2024. https://doi.org/10.1016/j.combustflame.2024.113892
73. S. B. Cronin, "Enhanced Photocatalysis on TiO2-Passivated III-V Compound Semiconductors and 2D Material Heterostructures for Water Splitting and CO2 Reduction," J. Electrochem. Soc., Aug. 2023. https://doi.org/10.1149/MA2023-01301802mtgabs
74. P. Priyandoko, "CO2-CH4 Hydrate Exchange: From Lab Kinetics to Reservoir-Scale Modeling," RG Experiments, Sep. 2025. https://doi.org/10.13140/RG.2.2.25460.82568
75. D. Ma, "Designing Hybrid Nanostructures for Enhancing Photon Harvest in Photocatalysis," J. Electrochem. Soc., Apr. 2018. https://doi.org/10.1149/MA2018-01/31/1866
76. R. R. Reddy, Y. N. Ahammed, K. Rama Gopal, and D. B. Basha, "Spectroscopic investigations on cometary molecules CO+, CH and CH+," J. Mol. Spectrosc., Apr. 2004. https://doi.org/10.1016/S0022-4073(03)00195-X
77. D. D. Bandara, K. L. Wickramasinghe, N. D. K. Dayawansa, R. P. De Silva, and M. I. M. Mowjood, "Application of Automated Floating Chamber to Quantify CO2 and CH4 Fluxes from Inland Freshwater Systems in Sri Lanka," Conf. Proc., Oct. 2025. https://doi.org/10.5281/zenodo.17270001
78. Okrah, G. Magara, C. Mensah, E. Yeboah, and N. A. Prempeh, "Quantifying anthropogenic impacts on CO2 and CH4 emissions: statistical insights and hotspot detection in East Africa," Environ. Monit. Assess., Jul. 2025. https://doi.org/10.1007/s10661-025-14361-3
79. S. Liu, J. Xiao, X. F. Lu, J. Wang, and X. Wang, "Electroreduction Efficient Electrochemical Reduction of CO2 to HCOOH over Sub-2nm SnO2 Quantum Wires with Exposed Grain Boundaries," Electrochim. Acta, Apr. 2019.
80. H. E. Ashoor and A. A. Dakhil, "Influence of Bi/Fe co-doping on the physical properties of anatase TiO2 nanoparticles," Sens. Mater., Nov. 2025. https://doi.org/10.1142/S3060932125500190
81. K. Li, S. Zhang, Y. Li, J. Fan, and K. Lv, "MXenes as noble-metal-alternative co-catalysts in photocatalysis," J. Mater. Sci., Jan. 2021. https://doi.org/10.1016/S1872-2067(20)63630-0
82. F. Xie and M. Schnell, "CO2 Versus CH4 Aggregation on Trifluorobenzene: Molecular Level

Characterization via Rotational Spectroscopy," Angew. Chem. Int. Ed., Sep. 2025. https://doi.org/10.1002/ange.202513517
83. J. Pan, B. Li, L. Dou, Y. Gao, and P. He, "Efficient CH3OH formation on H2/Ar plasma-treated CoO sites for CO2 + H2 + H2O DBD system," Plasma Process. Polym., Jul. 2023. https://doi.org/10.1002/ppap.202300069
84. D. Quang, T. Jen-Yu Liu, C. Chung, and Y.-C. Ling, "Photocatalytic reduction of CO2 on FeTiO3/TiO2 photocatalyst," Catal. Commun., Jan. 2012. https://doi.org/10.1016/j.catcom.2011.12.025
85. C. Li, W. Yang, L. Liu, W. Sun, and Q. Li, "In-situ Growth of TiO2 on TiN Nanoparticles for Non-noble-metal Plasmonic Photocatalysis," RSC Adv., Jul. 2016. https://doi.org/10.1039/C6RA15435B
86. Y. Cheng and R. Liu, "Designing of Pd1/TiO2-x Nanosheets for the Electrocatalyzed Reduction of CO2," J. Phys. Conf. Ser., Apr. 2023. https://doi.org/10.1088/1742-6596/2468/1/012162
87. M. Yang, H. Jin, and R. Gui, "Iron/cobalt co-doped boron quantum dots as nanozymes with peroxidase-like activities and the nanozyme-involved cascade catalysis system for ratiometric fluorescence and dual-mode visual detection of glutamate," Microchim. Acta, May 2025. https://doi.org/10.1007/s00604-025-07183-0
88. O. Jeznach, M. Gajc, A. Strzęp, W. Ryba-Rymanowski, and B. Surma, "Additional emission of bulk materials co-doped with CdTe quantum dots and silver nanoparticles," Poster, Apr. 2016.
89. T. Billoux, Y. Cressault, and A. Gleizes, "Tables of radiative transition probabilities for the main diatomic molecular systems of OH, CH, CH+, CO and CO+ occurring in CO–H2 syngas-type plasma," J. Quant. Spectrosc. Radiat. Transf., Jan. 2014. https://doi.org/10.1016/j.jqsrt.2013.09.005
90. P. G. Jones, J. Laube, and C. Thöne, "Organometallic Selenolates. 5.(1) Synthesis and Complexing Properties of 2-Propene- and 2-Methyl-2-propeneselenolato Molybdenum and Tungsten Compounds," 1997.
91. T. Tatsuma and H. Nishi, "Site-Selective Introduction of MnO2 Co-Catalyst to Gold Nanocubes for Enhanced Plasmonic Photocatalysis," Mater. Adv., Aug. 2023. https://doi.org/10.1149/MA2023-01141371mtgabs
92. M. Asif, L. Wang, P. Naveen, S. Nik, L. Randy, and R. Hazlett, "Influence of competitive adsorption, diffusion, and dispersion of CH4 and CO2 gases during the CO2-ECBM process," Fuel, Feb. 2024. https://doi.org/10.1016/j.fuel.2023.130065
93. Y. Li, C. Wang, M. Song, D. Li, and X. Zhang, "TiO2-x/CoOx photocatalyst sparkles in photothermocatalytic reduction of CO2 with H2O steam," Catal. Today, Dec. 2018.
94. K. K. Siddhapara, "Effect of Transition Metal (Fe, Co) Ion Doping on TiO2 Nanoparticles," Mater. Adv., Oct. 2022. https://doi.org/10.1149/MA2022-02382424mtgabs
95. Y. Zhang, Y. Wan, M. Wang, X. Bai, and Z. Zhang, "Efficient Electroreduction of CO2 to CH4 Over Amino Acid-Modified Copper Under Acidic Conditions," Chem. Biochem., Jul. 2025. https://doi.org/10.1002/cbh2.70005
96. D. Vrushabendrakumar, K. M. Alam, N. Chaulagain, N. Kumar, and K. Shankar, "Visible Light Driven CO2 Photoreduction Using TiO2 Nanotube Arrays Embedded with Low Bandgap Carbon Nitride Nanoparticles," Mater. Adv., Dec. 2023. https://doi.org/10.1149/MA2023-0291033mtgabs
97. Levi, A. Bansal, and D. Sasselov, "A High-pressure Filled Ice in the H2O–CO2–CH4 System, with Possible Consequences for the CO2–CH4 Biosignature Pair," Astrophys. J., Feb. 2023. https://doi.org/10.3847/1538-4357/acb49a
98. M. H. Foghani, O. Tavakoli, J. Parnian, and R. Zarghami, "Enhanced visible light photocatalytic CO2 reduction over direct Z-scheme heterojunction Cu/P co-doped g-C3N4@TiO2 photocatalyst," J. Mater. Sci., Jul. 2022. https://doi.org/10.1007/s11696-022-02109-z
99. S.-Y. Xu, W. Shi, J.-R. Huang, S. Yao, and C. Wang, "Single-cluster Functionalized TiO2 Nanotube Array for Boosting Water Oxidation and CO2 Photoreduction to CH3OH," Angew. Chem. Int. Ed., Jun. 2024. https://doi.org/10.1002/ange.202406223
100. K. Du, G. Liu, H. San, X. Chen, and K. Wang, "PbS Quantum Dots and Au Nanoparticle Co-Sensitized Black TiO2 Nanotubes for Photocurrent Enhancement," J. Electrochem. Soc., Sep. 2016. https://doi.org/10.1149/MA2016-02/12/1280
101. Mondal, M. Sultana, and A. Paul, "Understanding the mechanism of CO2 to CH4 conversion and hydrogen evolution reaction on Mg nanoparticles in water under ambient conditions: A DFT perspective," Int. J. Hydrogen Energy, Aug. 2025. https://doi.org/10.1016/j.ijhydene.2025.150978
102. Z. Y. Peng, Y. L. Liu, Y. Q. Cheng, K. Q. Chen, and P. Zhou, "Synthesis and photovoltaic properties of CuInS2/CdS quantum dots co-sensitised TiO2 photo-anodes," Int. J. Nanotechnol., Jan. 2014. https://doi.org/10.1504/IJNT.2014.063799
103. Q.-S. Chen, S.-G. Sun, Z.-Y. Zhou, Y.-X. Chen, and S.-B. Deng, "CoPt nanoparticles and their catalytic properties in electrooxidation of CO and CH3OH studied by in situ FTIRS," RSC Adv., Aug. 2008. https://doi.org/10.1039/b802047g
104. S. Y. Al-Qaradawi, A. F. Zedan, H. S. Rady, K. A. Soliman, and A. S. Aljaber, "Low-Temperature CO Oxidation Over CuO-TiO2 Nanocatalysts," QFARC Conf., Jan. 2016. https://doi.org/10.5339/qfarc.2016.EEPP1761

105. O. Baturina, A. P. Purdy, B. S. Simpkins, A. Epshteyn, and G. T. Forcherio, "Comparison of Photocatalytic Activities of TiN and Zrn Nanoparticles Incorporated into TiO2 matrix Under Visible Excitation," Mater. Adv., Sep. 2019. https://doi.org/10.1149/MA2019-02/45/2072
106. K. Takagi, Y. M. Hunge, I. Serizawa, and C. Terashima, "(Invited) Synthesis of TiO2-Based for Electrocatalysts CO2 Reduction Using in-Liquid Plasma Method and Control of Their Reduction Properties," Mater. Adv., Nov. 2024. https://doi.org/10.1149/MA2024-02684813mtgabs
107. P. J. Kulesza, A. Wadas, E. Szaniawska, R. Solarska, and K. Bienkowski, "Development of Nanostructured Hybrid Materials for Electrocatalytic and Photoelectrocatalytic Reduction of Carbon Dioxide," Mater. Adv., Jul. 2015. https://doi.org/10.1149/MA2015-02/43/1708
108. O. Baturina, J. Boltersdorf, A. Epshteyn, A. P. Purdy, and B. S. Simpkins, "(Invited) Comparison of Photocatalytic Activities of TiN and Zrn Nanoparticles Incorporated into TiO2 matrix Under Visible Excitation," Mater. Adv., May 2020. https://doi.org/10.1149/MA2020-01512803mtgabs
109. T. Ishiku, S. Kamimura, and T. Ohno, "Photoanode-Driven Photoelectrochemical CO2 Reduction By Using the TiO2 Photoanodes and Different Metal Counter Electrodes (Pt, Ti, Cu, Sn, Zn)," Mater. Adv., Sep. 2016. https://doi.org/10.1149/MA2016-02/49/3659
110. P. Challa, V. R. M. Peddinti, N. Ajmeera, and D. Raju B., "Coupling of CH3OH and CO2 with 2-cyanopyridine for enhanced yields of dimethyl carbonate over ZnO–CeO2 catalyst," J. Chem. Sci., Aug. 2019. https://doi.org/10.1007/s12039-019-1651-4
111. O. Baturina, J. Boltersdorf, A. Epshteyn, A. P. Purdy, and B. S. Simpkins, "Comparison of Photocatalytic Activities of TiN and Zrn Nanoparticles Incorporated into TiO2 matrix Under Visible Excitation," Mater. Adv., Nov. 2020. https://doi.org/10.1149/MA2020-02613103mtgabs
112. H. Zhao, W. Wang, X. Li, P. Li, and M. Cai, "Engineering the Interfacial Structure of Heavy Metal-Free Colloidal Heterostructured Quantum Dots for High-Efficiency Photoelectrochemical Water Oxidation without Co-Catalyst," Adv. Eng. Sci. Res., Dec. 2022. https://doi.org/10.1002/aesr.202200142
113. L.-q. Yu, R.-t. Guo, C. Xia, S.-h. Guo, and J.-s. Yan, "Bismuth-Metal and Carbon Quantum Dot Co-Doped NiAl-LDH Heterojunctions for Promoting the Photothermal Catalytic Reduction of CO2," Small, Dec. 2024. https://doi.org/10.1002/smll.202409901
114. W.-G. Cui, G.-Y. Zhang, T.-L. Hu, and X.-H. Bu, "Metal-organic framework-based heterogeneous catalysts for the conversion of C1 chemistry: CO, CO2 and CH4," Coord. Chem. Rev., May 2019. https://doi.org/10.1016/j.ccr.2019.02.001
115. J. Pan, B. Li, L. Dou, Y. Gao, and P. He, "Efficient CH3OH formation on H2/Ar plasma-treated CoO sites for CO2 + H2 + H2O DBD system," Plasma Process. Polym., Jul. 2023. https://doi.org/10.1002/ppap.202300069
116. V. M. Dubin, A. L. Gindilis, B. L. Walton, S. R. Bauers, and A. Albrecht, "Electroless Metallization of Dielectric Surfaces," Mater. Adv., Sep. 2016. https://doi.org/10.1149/MA2016-02/18/1528
117. F. Rathmann, I. M. Abdelsalam, S. Wang, M. M. Kubik, and S. Frindy, "Plasmon-Enhanced CO2 Methanation over Au@Ru/TiO2 via Nanoscale Control of Ru Shell Thickness," Angew. Chem. Int. Ed., Nov. 2025. https://doi.org/10.1002/ange.202518748
118. T. Yamamoto, H. Katsumata, T. Suzuki, and S. Kaneco, "Conversion of CO2 in Methanol into HCOOCH3 and CO By Photoelectrochemical Reduction with TiO2 Photoanode," Mater. Adv., Sep. 2016. https://doi.org/10.1149/MA2016-02/49/3665
119. X. Zhang, W. Zou, and J. Duan, "Enhanced Photovoltaic Performance of CdSe Quantum Dot-Sensitized Solar Cells Utilizing Sm–Eu Co-Doped TiO2 Photoanodes," IEEE Trans. Electron Devices, Jan. 2025. https://doi.org/10.1109/TED.2025.3622562
120. E. B. Creel, Y. Kim, E. R. Corson, F. Qiu, and R. Kostecki, "Plasmon-Enhanced Photocatalytic CO2 Reduction Using Colloidal Nanocrystals," Mater. Adv., Sep. 2016. https://doi.org/10.1149/MA2016-02/49/3603
121. T. Spataru, M. Marcu, and N. Spataru, "Electrocatalytic and photocatalytic activity of Pt-TiO2 films on boron-doped diamond substrate," Poster, May 2012.
122. S. I. Khan, L. Heymès, M. S. E. Houache, Y. A. Abu-Lebdeh, and E. A. Baranova, "Plasmonic Cu/ZnO Catalysts for CO2 Electrochemical Reduction," Mater. Adv., Jul. 2025. https://doi.org/10.1149/MA2025-01522561mtgabs
123. Y. Liu, C.-C. Lee, M. W. Horn, and H. Lee, "Toward efficient photocatalysts for light-driven CO2 reduction: TiO2 nanostructures decorated with perovskite quantum dots," J. Phys. Energy, Apr. 2021. https://doi.org/10.1088/2632-959X/abf3d2
124. O. Baturina, B. S. Simpkins, J. Boltersdorf, A. Epshteyn, and A. P. Purdy, "(Invited) Photoelectrochemical Methanol Oxidation Under Visible and UV Excitation of TiO2-Supported TiN and Zrn Plasmonic Nanoparticles," Mater. Adv., May 2021. https://doi.org/10.1149/MA2021-01471929mtgabs
125. F. Yu, G. Zhang, M. Shu, and H. Wang, "f–π* Back-Bonding Orbital Induced by a Lutetium-Based Conducting Metal–Organic Framework Promotes

Highly Selective CO2-to-CH4 Conversion at Low Potential," Angew. Chem. Int. Ed., Nov. 2024. https://doi.org/10.1002/ange.202416467
126. J. J. Concepcion, J. W. Jurss, M. K. Brennaman, P. G. Hoertz, and A. O. T. Patrocinio, "Making Oxygen with Ruthenium Complexes," Acc. Chem. Res., Oct. 2009. https://doi.org/10.1021/ar9001526
127. O. Baturina, A. Epshteyn, and B. S. Simpkins, "Photoelectrochemical Methanol Oxidation on TiN@Au Core-Shell Nanoparticles Supported on TiO2," Mater. Adv., Jul. 2018. https://doi.org/10.1149/MA2018-02/54/1938
128. Ali and W.-C. Oh, "Synthesis of Ag2Se–graphene–TiO2 nanocomposite and analysis of photocatalytic activity of CO2 reduction to CH3OH," J. Sci. Ind. Res., Nov. 2017. https://doi.org/10.1007/s12034-017-1494-x
129. D. H. Kim, Y. H. Jang, S. T. Kochuveedu, and L. N. Quan, "Plasmonic Solar Fuels Based on Nanostructured Oxide Photocatalysts," Mater. Adv., Aug. 2014. https://doi.org/10.1149/MA2014-02/8/563
130. T. Tatsuma, "(Invited) Plasmonic Photocatalysis and Near-Field Photocatalysis," Mater. Adv., Nov. 2024. https://doi.org/10.1149/MA2024-02684810mtgabs
131. G. Pareras, V. Cabedo, M. R. S. McCoustra, and A. Rimola, "Single-atom catalysis in space II. Ketene–acetaldehyde–ethanol and methane synthesis via Fischer-Tropsch chain growth," Astron. Astrophys., May 2024. https://doi.org/10.1051/0004-6361/202449378
132. G. Yan, P. Pršlja, G. Chen, J. Kang, and Y. Liu, "Syngas conversion to higher alcohols via wood-framed Cu/Co-carbon catalyst," arXiv Preprint, May 2024. https://doi.org/10.48550/arXiv.2405.15526
133. M. K. Hussain and T. Iqbal, "Critical Review on Modification of TiO2 for the Reduction of CO2," Mater. Adv., Sep. 2019.
134. H. Park, "(Invited) Solar Synthesis of C1-C4 Chemicals from Carbon Dioxide and Water," Mater. Adv., Sep. 2016. https://doi.org/10.1149/MA2016-02/49/3690
135. L. Calantropo, E. La Greca, L. F. Liotta, G. Impellizzeri, and A. Gulino, "Solar photothermo-catalytic CO2 conversion into methane: Effect of phyllosilicates on the performance of Ni-Zn-Al layered double hydroxide-derived catalysts," J. CO2 Util., Dec. 2025. https://doi.org/10.1016/j.jcou.2025.103302
136. M. Yagi, "(Invited) Synthetic Catalysts for Water Oxidation Using Metal Complexes and Nanoparticles," Mater. Adv., Jul. 2018. https://doi.org/10.1149/MA2018-03/4/268
137. T. Zhang, W. Li, K. Huang, H. Guo, and Z. Li, "Regulation of functional groups on graphene quantum dots directs selective CO2 to CH4 conversion," Nat. Commun., Sep. 2021. https://doi.org/10.1038/s41467-021-25640-1
138. S. Li, Z. Ma, X. Zhong, B. Wu, and J. Guo, "Hydrogen Spillover-Mediated Spatial Decoupling Process Boosts Syngas Conversion to Higher Oxygenates," J. Am. Chem. Soc., Dec. 2025. https://doi.org/10.1021/jacs.5c14341
139. Y. Xiao, Y. Xu, Y. Ding, and H. Huang, "Engineered Microenvironment of Imidazolium Salts by Multi-scale Modeling and Machine Learning Algorithms for Enhanced Electrocatalytic CO2 Reduction to Ethylene and Acetamide via Targeted Delivery of CuAg Alloy Tandem Catalyst Based on Cu(111) Facet," RSOS Preprint, May 2025. https://doi.org/10.21203/rs.3.rs-6647633/v1
140. N. Joshi and S. Loganathan, "In Situ Modification of CuO−Fe2O3 by Nonthermal Plasma: Insights into the CO2-to-CH3OH Hydrogenation Reaction," ACS Omega, Mar. 2023. https://doi.org/10.1021/acsomega.3c00915
141. W.-H. Bai, Q. Shao, Y.-K. Ji, H. Dong, and X.-Y. Hu, "Pd─N4 Sites in MOFs Modulate Oxygen Reduction Pathways for 100% Selective Photocatalytic CO2-to-CH4 Conversion from Oxygenated Flue Gas," Angew. Chem. Int. Ed., Oct. 2025. https://doi.org/10.1002/ange.202513157
142. M. Zhi, "(Invited) Plasmonic Aerogels for Gas-Phase Photocatalytic Reactions," Mater. Adv., Dec. 2023. https://doi.org/10.1149/MA2023-02472350mtgabs
143. K. Tanaka, Y. Kushi, K. Tsuge, K. Toyohara, and T. Nishioka, "Catalytic Generation of Oxalate through a Coupling Reaction of Two CO2 Molecules Activated on [(Ir(η5-C5Me5))2(Ir(η4-C5Me5)CH2CN)(μ3-S)2]," J. Organomet. Chem., Feb. 1998.
144. O. Baturina, A. Epshteyn, A. C. Leff, A. P. Purdy, and T. H. Brintlinger, "Photoelectrochemical Methanol Oxidation Under Visible and UV Excitation of TiO2-Supported TiN and ZrN Plasmonic Nanoparticles," Mater. Adv., Jan. 2021. https://doi.org/10.1149/1945-7111/abd605
145. Y. M. Davydenko, "SYNTHESIS AND CHARACTERIZATION OF COORDINATION COMPOUNDS OF TRANSITION METALS BASED ON 5-METHYL-3-(TRIFLUOROMETHYL)-1H-PYRAZOLE," J. Coord. Chem., Dec. 2025. https://doi.org/10.17721/1728-2209.2025.1(60).10
146. M. Ezzeddine, K. Harb, J. Wang, and E. A. Baranova, "Unraveling the Role of Lithium-Ion Promotion in Iridium and Platinum Catalysts for CO Oxidation," Mater. Adv., Jul. 2025. https://doi.org/10.1149/MA2025-01623040mtgabs
147. V. S. Kashansky, "Microwave-assisted synthesis of M/TiO2/C (M=Ni, Cu, Ni–Cu) photocatalysts for CO2 reduction: structural evolution and photocatalytic properties," Mater. Adv., Jan. 2026.

https://doi.org/10.17586/2220-8054-2025-16-6-865-871
148. M. A. Hossen, R. R. Ikreedeegh, A. A. Aziz, and M. Tahir, "Comparative study on photocatalytic CO2 reduction performance of modified-TiO2 nanotube arrays," Nano Mater., Jul. 2025. https://doi.org/10.1016/j.nxmate.2025.100951
149. Kempi, R. Verma, A. K. Sharma, and F. Mauss, "CO2 methanation: a review on optimizing catalysts and conditions," React. Kinet. Mech. Catal., Feb. 2026. https://doi.org/10.1007/s11144-026-03040-0
150. P. J. Kulesza and I. A. Rutkowska, "(Invited) Stabilization and Activation of Copper(I)-Oxide-Semiconducting Interfaces for Photoelectrochemical Reduction of Carbon Dioxide," Mater. Adv., Dec. 2023. https://doi.org/10.1149/MA2023-02472360mtgabs
151. K. Du, G. Liu, X. Chen, and K. Wang, "High-Efficiency Photocatalysts for CO2 Conversion Based on MoS2/CdS/TiO2 Nanotubes Heterostructures," Mater. Adv., Apr. 2018. https://doi.org/10.1149/MA2018-01/28/1621
152. Y. Ni, W. Xie, Z. Yan, F. Cheng, and J. Chen, "Spatially-Directed C─C Coupling inside Three-dimensional Metal-organic Frameworks for CO2 Electroreduction to C2 Products," Angew. Chem. Int. Ed., Oct. 2025. https://doi.org/10.1002/ange.202518398
153. J. Mao, L. Ye, K. Li, X. Zhang, and J. Liu, "Pt-loading reverses the photocatalytic activity order of anatase TiO2 {001} and {010} facets for photoreduction of CO2 to CH4," Appl. Catal. B, Aug. 2014. https://doi.org/10.1016/j.apcatb.2013.08.027
154. M. Esmaeilirad, A. Kondori, A. R. Belmonte, and M. Asadi, "Electroreduction of Carbon Dioxide to Methane Enabled By Molybdenum Carbide Nanocatalyst," Mater. Adv., Nov. 2020. https://doi.org/10.1149/MA2020-02633234mtgabs
155. Al-Zubeidi, B. Bourgeois, A. Dai, L. Herndon, and L. Yuan, "Plasmon-Assisted Electrochemical CO2 Reduction on Copper Nanocubes," Mater. Adv., Nov. 2024. https://doi.org/10.1149/MA2024-02594034mtgabs
156. L. Duranti, U. P. Laverdura, M. L. Grilli, and E. DiBartolomeo, "Coking Resistant DRM Active Ru-Loaded Calcium Zirconate for Applications at SOC Fuel Electrode," Mater. Adv., Nov. 2025. https://doi.org/10.1149/MA2025-031157mtgabs
157. G. Yin, H. Abe, E. Sakai, and M. Miyauchi, "A Cu-Zn Intermetallic Catalyst Utilized for Electrochemical, Photoelectrochemical and Photocatalytic CO2 Reduction," Mater. Adv., Sep. 2016. https://doi.org/10.1149/MA2016-02/49/3601
158. Q. Zhu, C. Wang, H. Ren, M. Zeng, and Z. Kan, "Conversion of water and carbon dioxide into methanol with solar energy on Au/Co nanostructured surfaces," Mater. Adv., Mar. 2020. https://doi.org/10.1088/2053-1591/ab7d0e
159. T. Oshikiri, "(Invited) Nitrogen Fixation Under Modal Coupling Regime between Plasmon and Optical Cavity Modes," Mater. Adv., Nov. 2025. https://doi.org/10.1149/MA2025-02472344mtgabs
160. C. Xie, F. Lv, X. Wu, X. Wang, and Y. Yu, "Simultaneous Enhancement of Photocatalytic CH4 Conversion and H2O2 Production through Water Confinement in Nanoporous Core-Shell Catalysts," RSOS Preprint, Apr. 2025. https://doi.org/10.21203/rs.3.rs-6469567/v1
161. H. Nawaz, G. Hussain, E. Qazi, S. Naz, and J. Zimba, "Ultrafast Photo-Electrocatalytic Nanoparticle Networks for Dual CO2 Reduction and High-Energy Storage in Hybrid Quantum Materials," Sci. J. Light Sci., Nov. 2025. https://doi.org/10.36348/sjls.2025.v10i10.005
162. S. Liu, J. Xiao, X. F. Lu, J. Wang, and X. Wang, "Electroreduction Efficient Electrochemical Reduction of CO2 to HCOOH over Sub-2 nm SnO2 Quantum Wires with Exposed Grain Boundaries," J. Electrochem., Apr. 2019.
163. K. Sun, Z. Liu, F. Song, H. Feng, and L. Shao, "Tailoring oxygen vacancies in NiAl catalysts via different synthesis methods dictates performance in CO2 dry reforming of methane," Int. J. Hydrogen Energy, Oct. 2025. https://doi.org/10.1016/j.ijhydene.2025.152202
164. S. Liu, J. Xiao, X. F. Lu, J. Wang, and X. Wang, "Electroreduction Efficient Electrochemical Reduction of CO2 to HCOOH over Sub-2nm SnO2 Quantum Wires with Exposed Grain Boundaries," 2019.
165. D. Quang, T. Liu, C.-C. Chung, and Y.-C. Ling, "Photocatalytic reduction of CO2 on FeTiO3/TiO2 photocatalyst Keywords: FeTiO3 TiO2 CO2 reduction CH3OH Visible light response," Catal. Commun., Jan. 2012. https://doi.org/10.1016/j.catcom.2011.12.025
166. Qasim, M., Manzoor, S., Nabeel, M. I., Hussain, S., Waqas, R., Joseph, C. G., & Suazo-Hernández, J. (2025). Harnessing High-Valent Metals for Catalytic Oxidation: Next-Gen Strategies in Water Remediation and Circular Chemistry. *Catalysts*, *15*(12), 1168. https://doi.org/10.3390/catal15121